

# Dissipative quantum generative adversarial networks

Kerstin Beer <sup>\*</sup>      Gabriel Müller <sup>†</sup>

December 14, 2021

Noisy intermediate-scale quantum (NISQ) devices build the first generation of quantum computers. Quantum neural networks (QNNs) gained high interest as one of the few suitable quantum algorithms to run on these NISQ devices. Most of the QNNs exploit supervised training algorithms with quantum states in form of pairs to learn their underlying relation. However, only little attention has been given to unsupervised training algorithms despite interesting applications where the quantum data does not occur in pairs. Here we propose an approach to unsupervised learning and reproducing characteristics of any given set of quantum states. We build a generative adversarial model using two dissipative quantum neural networks (DQNNs), leading to the dissipative quantum generative adversarial network (DQGAN). The generator DQNN aims to produce quantum states similar to the training data while the discriminator DQNN aims to distinguish the generator's output from the training data. We find that training both parts in a competitive manner results in a well trained generative DQNN. We see our contribution as a proof of concept for using DQGANs to learn and extend unlabeled training sets.

The last years brought forth the first generation of quantum computers, namely, noisy intermediate-scale quantum (NISQ) devices [1–3]. These devices are limited by high noise levels and a small number of qubits. Additionally, the noise limits the quantum circuits to only short depth before the signal-to-noise ratio becomes too small. Due to these limitations, today's quantum computers do not achieve fault-tolerant quantum computation [4, 5]. However, this is required to perform promising applications [6] such as Shor's factoring algorithm [7] or quantum simulation [8].

---

<sup>\*</sup>Institut für Theoretische Physik, Leibniz Universität Hannover, Appelstraße 2, 30167 Hannover, Germany, kerstin.beer@itp.uni-hannover.de

<sup>†</sup>previously Institut für Theoretische Physik, presently Institut für Quantenoptik, Leibniz Universität Hannover, Welfengarten 1, 30167 Hannover, Germany, g.mueller@iqo.uni-hannover.de

Quantum Neural Networks (QNNs) belong to the few quantum algorithms that can be executed on NISQ devices [9]. A QNN can be implemented as a hybrid quantum-classical algorithm [10–13]. It executes a short parameterised quantum circuit (PQC) [14–16] on a quantum computer while optimising its parameters classically. This process saves important resources such that these QNNs can also work under the limitations of NISQ devices [17].

Here, we focus on the dissipative QNN (DQNN) [18] which features a unique set of qubits for each network layer. It is universal for quantum computation and has achieved remarkable results for various applications [19, 20], including their application on actual NISQ devices [17]. The DQNN propagates the input state’s information through the network in a feed-forward manner. This is realized through completely positive layer-to-layer transition maps that act on the qubits of two adjacent layers. Each qubit is characterised by an individual quantum perceptron unitary, the fundamental building block of the DQNN.

Most of the current QNN applications are limited to supervised learning of labeled training states [9]. This includes their use for classification [21–23], denoising quantum data [19, 24–27], learning unitary transformations [17, 18, 28–31] and learning graph-structured quantum data [20, 30–34]. In these problems, the QNNs are trained with respect to a special family of loss functions. These compare the network’s output state for each input state to the respective target output state. However, there are problems where these training pairs do not exist and a different approach is required for training.

We introduce dissipative quantum generative adversarial networks (DQGANs) for unsupervised learning of an unlabeled training set. The fundamental concept is adopted from the highly successful classical generative adversarial networks [35]. One DQGAN consists of two DQNNs, namely, the generator and the discriminator. The discriminator’s aim is to distinguish real training states from fake states produced by the generator. The generator’s aim is to produce fake states that the discriminator can not distinguish from the real ones. By alternately and adversarially training the networks the generator should learn the relevant features of the training set and produce states that extend the training set.

Our aim with the DQGAN is to extend a given unlabeled training set featuring any desired quantum states. The current literature on generative adversarial learning with QNNs mainly aimed and achieved to reproduce labeled training states [36, 37]. However, this neglects their major potential to produce states similar to a set of unlabeled training states without the need of any further information. The latter usage enables a whole range of exciting possibilities. For example, the DQGAN could be trained on a limited set of naturally produced quantum states and learn to produce similar quantum states for any imaginable further use in the future.

We realise the DQGAN in two ways, once by a simulation on a classical computer, another time by simulating a concrete quantum circuit implementation. The first one allows a direct implementation of the quantum perceptron unitaries. These can effectively be trained by the later introduced quantum backpropagation algorithm. However, this implementation requires information that is not accessible during the execution on a NISQ device. Therefore, we additionally provide a concrete quantum circuit imple-

mentation (DQGAN<sub>Q</sub>) which is trained by the gradient descent algorithm.

In contrast to some proposals of *quantum generative adversarial networks* (QGANs) [36–45] DQGAN is a fully quantum architecture and is trained with quantum data. In [42, 43], for example, QGANs are defined as quantum-classical hybrid and include a quantum generator and a classical discriminator. Moreover, the authors of [38] present the usage of quantum or classical data and two quantum processors in an adversarial learning setting. Furthermore, some of the QGAN proposals are trained with labelled data [36]. In contrary the here proposed DQGAN can be trained with a set of unlabelled quantum states, to which only the discriminative model has access.

In this work, we provide proof of concept for using DQGANs to learn and extend an unlabeled training set. We train the DQGAN on two different toy models, a set of quantum states forming a line on the Bloch sphere and another set of clustered quantum states. Here, we succeed on showing the vast potential of our DQGAN implementations.

Our paper is organized as follows: in Section 1, we describe the general concepts of our DQNN and follow up with the definitions of its two implementations. In Section 2, we introduce the general concept of generative adversarial training with DQNNs, leading to the DQGAN and a concrete training algorithm. Conclusively, we present our results in Section 3 and discuss their relevance to the field in Section 4.

## 1 Quantum neural networks

Many attempts on building a QNN, the quantum analogue of the popular classical neural network, have been made [18, 22, 23, 25, 46–60]. In the following we describe the architecture of so-called *dissipative quantum neural networks* (DQNNs) [17, 18, 20] as we will exploit this ansatz to form the DQGANs. We explain how their training algorithm can be simulated on a classical computer and how the DQNN can be implemented on a quantum computer [20].

### 1.1 Dissipative quantum neural network

DQNNs are build of layers of qubits, which are connected via building blocks. Such a building block, named perceptron, is engineered as an arbitrary unitary operation. We can express the propagation of a state  $\rho^{\text{in}}$  trough the network as a composition of layer-to-layer transition maps, namely

$$\rho^{\text{out}} = \mathcal{E}(\rho^{\text{in}}) = \mathcal{E}^{L+1}(\mathcal{E}^L(\dots \mathcal{E}^2(\mathcal{E}^1(\rho^{\text{in}})) \dots)), \quad (1)$$

where the transition maps are defined as

$$\mathcal{E}^l(X^{l-1}) \equiv \text{tr}_{l-1} \left( \prod_{j=m_l}^1 U_j^l(X^{l-1} \otimes |0\dots 0\rangle_l \langle 0\dots 0|) \prod_{j=1}^{m_l} U_j^{l\dagger} \right),$$

where  $U_j^l$  refers to the  $j$ th perceptron acting on layers  $l-1$  and  $l$ , and  $m_l$  is the total number of perceptrons connecting layers  $l-1$  and  $l$ , see Fig. 1a. These maps tensor the

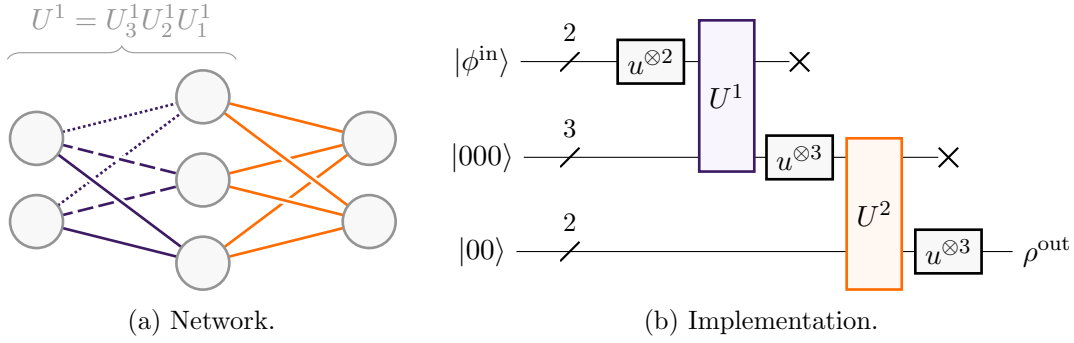


Figure 1: **DQNN** An exemplary DQNN consisting of two layers of quantum perceptrons (a) can be implemented as quantum circuit (b). The  $u$ -gates represent layers of single qubit operations.  $U^l = U_{m_l}^l \dots U_1^l$  denote the layer unitaries, where every unitary  $U_k^l$  is expressed through two-qubit unitaries, see [18].

state of the current layer to the state of the next layer's qubits and apply the perceptron unitaries. Since the qubits from the first of the two layers are traced out additionally, these QNNs are called *dissipative*.

The training of such a QNN architecture is done with respect to a data set containing  $S$  input and desired output states, namely  $\{|\phi_x^{\text{in}}\rangle, |\phi_x^{\text{SV}}\rangle\}$ . For example, in [18] it is shown that the DQNN algorithm can successfully characterize an unknown unitary  $Y$ , using desired output training states of the form  $|\phi_x^{\text{SV}}\rangle = Y |\phi_x^{\text{in}}\rangle$ .

Generally, the training is done via maximising a training loss function based on the fidelity  $F$  of two states, e.g., of the form

$$\mathcal{L}_{\text{SV}} = \frac{1}{S} \sum_{x=1}^S F(|\phi_x^{\text{SV}}\rangle \langle \phi_x^{\text{SV}}|, \rho_x^{\text{out}}) = \frac{1}{S} \sum_{x=1}^S \langle \phi_x^{\text{SV}} | \rho_x^{\text{out}} | \phi_x^{\text{SV}} \rangle. \quad (2)$$

The general aim is to optimise such a loss function by updating the variable parts of the DQNN. In the following we explain the training process in two cases, the simulation on a classical computer and the quantum circuit implementation suitable for NISQ devices.

## 1.2 Classical simulation implementation

We can implement the algorithm using the quantum perceptron unitaries  $U_j^l$  directly. Hence, every perceptron is described via  $(2^{m_l+1})^2 - 1$  parameters. Via feed-forward propagation of the input state through the DQNN and back-propagation of the desired output state we can gain information on how every unitary  $U_j^l$  has to be updated to minimize the training loss, exemplary defined in Eq. (2). We can formulate the update,

using an update matrix  $K_j^l(t)$ , as

$$U_j^l(t + \epsilon) = e^{i\epsilon K_j^l(t)} U_j^l(t),$$

where  $\epsilon$  is the training step size and  $t$  is the step parameter. The concrete formula of the update matrix is derived in [18]. Remarkable is, that to evaluate the matrix  $K_j^l(t)$ , which updates a perceptron connecting layers  $l - 1$  and  $l$ , only two quantum states are needed: the output state of layer  $l$  obtained by feed-forward propagation through the network, and the state of the layer  $l + 1$  obtained by back-propagation of the desired output. For more details of the classical simulation of a DQNN algorithm we point to [18]. The code can be found at [61].

### 1.3 Quantum circuit implementation

To implement the quantum perceptrons on a quantum computer we have to abstract the perceptron unitaries into parameterised quantum gates. In [17] it is used that every arbitrary two-qubit unitary can be implemented with a two-qubit canonical gate and single qubit gates, see [62–67]. This yields the implementation of each perceptron via  $m_{l-1}$  two-qubit unitaries connecting one qubit of the output layer  $l$  to all qubits in the input layer  $l - 1$ , respectively.

Rephrasing the sequence of single qubit gates in form of the gate  $u$  and summarizing the two-qubit canonical gates in  $U^l$  leads to the neat representation in Fig. 1b. For the DQNN<sub>Q</sub>,  $n = \sum_{l=1}^L m_l$  qubits are needed, where  $L$  is the number of layers. The overall PQC consists of  $3m + 3 \sum_{l=1}^{L+1} m_{l-1}(1 + m_l)$  parameters.

The DQNN<sub>Q</sub> implementation can be trained with gradient descent. At the beginning, the parameters of the quantum circuit are initialised as  $\vec{\omega}_0$ . All parameters are updated by  $\vec{\omega}_{t+1} = \vec{\omega}_t + \vec{d}\omega_t$  in every training epoche, where  $\vec{d}\omega_t = \eta \nabla \mathcal{L}_{SV}(\vec{\omega}_t)$  with the learning rate  $\eta$  and the gradient is of the form

$$\nabla_k \mathcal{L}_{SV}(\vec{\omega}_t) = \frac{\mathcal{L}_{SV}(\vec{\omega}_t + \vec{e}_k) - \mathcal{L}_{SV}(\vec{\omega}_t - \vec{e}_k)}{2\epsilon} + \mathcal{O}(\epsilon^2).$$

For a thorough explanation of the DQNN<sub>Q</sub> suitable for the execution on NISQ devices we refer to Appendix B and [17].

## 2 Dissipative quantum adversarial neural networks

In the field of machine learning we can generally distinguish *discriminative* and *generative* models. For instance, classification problems such as classifying handwritten digits [68] are common discriminative tasks. On the contrary, generative models produce data. Speaking in the example of handwritten digits, we would train a generative model to produce different “handwritten” digits from random input.

In the following, we describe *generative adversarial networks* (GANs). These are built of two models, where one of them has a generative and the other one a discriminative

task. It is much harder to train generative models than discriminative models. The proposal of GANs offered new possibilities and has since found a lot of applications [69], ranging from classification or regression tasks [69–71] to the generation [72] and improvement [73] of images.

## 2.1 General concept

GANs were first introduced in [35]. The generative and discriminative parts of their GAN are implemented as a multi-layer perceptron, respectively. On the one hand, the generative model gets random noise samples as input and produces synthetic samples. On the other hand, the discriminator has access to both the generator’s output and samples from the training data. In the original proposal, this data cannot be accessed by the generator.

The training aim of the discriminator is to distinguish correctly between the training data and the synthetic data. Since the generator’s goal is to trick the discriminative model, the problem is called a *minimax problem*.

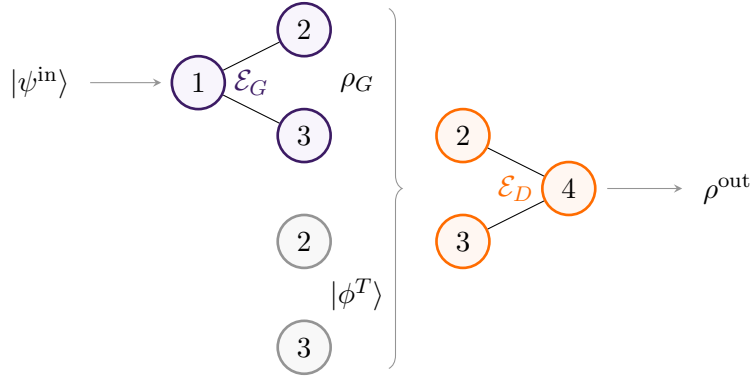


Figure 2: **DQGAN**. The depicted DQGAN consists of four qubits. Qubits 2 and 3 are shared by the generative and the discriminative QNN. The state of this qubits is either the generator’s output state  $\rho_G$  on the input state, i.e.,  $\rho_G = \mathcal{E}_G(|\psi^{\text{in}}\rangle \langle\psi^{\text{in}}|)$  or a given training state  $|\phi^T\rangle$ .

Following the above-described ansatz, the DQGAN is constructed of two DQNNs, the generative model, and the discriminative model, described through the completely positive maps  $\mathcal{E}_G$  and  $\mathcal{E}_D$ , respectively. The number of qubits in the generator’s last layer equals the number of qubits in the discriminator’s first layer. Hence, the generator’s output can be used as input for the discriminator.

For the training a set of training states  $\{|\phi_x^T\rangle\}_{x=1}^N$  and a set of random states  $\{|\psi_x^{\text{in}}\rangle\}$  is used. We assume the the states of both sets to be pure. The overall goal is to adversarially train both DQNNs, so that the generator produces states with characteristics similar to the training data. We can describe the output of the discriminator DQNN as

$$\rho^{\text{out}} = \begin{cases} \mathcal{E}_D(\mathcal{E}_G(|\psi^{\text{in}}\rangle \langle \psi^{\text{in}}|)) & \text{for generated data} \\ \mathcal{E}_D(|\phi^T\rangle \langle \phi^T|) & \text{for training data.} \end{cases}$$

To be more precise we shortly discuss the DQGAN depicted in Fig. 2 and consisting of four qubits. Please consider Fig. 1 for a better understanding of the following description. The generative model consists of two two-qubit unitaries  $U_{G1}$  and  $U_{G2}$ , acting on qubits 1 and 2, and qubits 1 and 3, respectively. The discriminator is described by a single three-qubit unitary  $U_D$ . If the discriminative model gets a training data state  $|\phi^T\rangle$  as input the resulting discriminator output state can be described as

$$\rho_{\text{out}}^D = \text{tr}_{\{2,3\}} \left( U_D (|\phi^T\rangle \langle \phi^T| \otimes |0\rangle \langle 0|) U_D^\dagger \right).$$

For the the generator's output as input, the discriminator has the output

$$\rho_{\text{out}}^{G+D} = \text{tr}_{\{1,2,3\}} \left( U_D U_{G2} U_{G1} (|\psi_x^{\text{in}}\rangle \langle \psi_x^{\text{in}}| \otimes |000\rangle \langle 000|) U_{G1}^\dagger U_{G2}^\dagger U_D^\dagger \right).$$

The general form of these output states is used in the proof of Proposition 1.

The original DQNN approach focuses on characterising a relation between input and output data pairs. However, we try to characterise a data set of single quantum states instead. We aim to train a generative model in a way that it is able to produce quantum states with similar properties compared to the training data set. Such extended quantum data sets can be, for example, useful for experiments or training other QNN architectures.

## 2.2 Training algorithm

In analogy to the classical case described in [35] we can describe the training process through

$$\min_G \max_D \left( \frac{1}{S} \sum_{x=1}^S \langle 0 | \mathcal{E}_D(\mathcal{E}_G(|\psi_x^{\text{in}}\rangle \langle \psi_x^{\text{in}}|)) | 0 \rangle + \frac{1}{S} \sum_{x=1}^S \langle 1 | \mathcal{E}_D(|\phi_x^T\rangle \langle \phi_x^T|) | 1 \rangle \right). \quad (3)$$

The updates of the discriminator and the generator take place alternately. For updating the generator we maximise the loss function

$$\mathcal{L}_D(\mathcal{E}_D, \mathcal{E}_G) = \frac{1}{S} \sum_{x=1}^S \langle 0 | \mathcal{E}_D(\mathcal{E}_G(|\psi_x^{\text{in}}\rangle \langle \psi_x^{\text{in}}|)) | 0 \rangle + \frac{1}{S} \sum_{x=1}^S \langle 1 | \mathcal{E}_D(|\phi_x^T\rangle \langle \phi_x^T|) | 1 \rangle$$

for  $r_D$  rounds, whereas the generator is trained through maximising

$$\mathcal{L}_G(\mathcal{E}_D, \mathcal{E}_G) = \frac{1}{S} \sum_{x=1}^S \langle 1 | \mathcal{E}_D(\mathcal{E}_G(|\psi_x^{\text{in}}\rangle \langle \psi_x^{\text{in}}|)) | 1 \rangle.$$

assume for  $r_G$  rounds. Note that  $\mathcal{L}_G$  differs from the corresponding term in Eq. (3) in that the fidelity is calculated with respect to  $|1\rangle$  instead of  $|0\rangle$ . Therefore, the generator is trained by maximising  $\mathcal{L}_G$  rather than minimising. These procedures are repeated for  $r_T$  epochs. The overall training algorithm is described in Algorithm 1.

---

**Algorithm 1** Training of the DQGAN.

---

```

initialize network unitaries
for  $r_T$  epochs do
    make a list of  $S$  randomly chosen states of the training data list  $\{|\phi_x^T\rangle\}_{x=1}^N$ 
    for  $r_D$  epochs do
        make a list of  $S$  random states  $|\psi_x^{\text{in}}\rangle$ 
        update the discriminator unitaries by maximizing  $\mathcal{L}_D$ 
    end for
    for  $r_G$  epochs do
        make a list of  $S$  random states  $|\psi_x^{\text{in}}\rangle$ 
        update the generator unitaries by maximising  $\mathcal{L}_G$ 
    end for
end for
make a list of  $V$  random states  $|\psi_x^{\text{in}}\rangle$ 
propagate each  $|\psi_x^{\text{in}}\rangle$  through the generator to produce  $V$  new states
calculate  $\mathcal{L}_V$ 

```

---

**Proposition 1.** *The update matrix for a QGAN trained with pure states  $|\phi_x^T\rangle$  has to be of the form*

$$K_j^l(t) = \frac{\eta 2^{m_{l-1}i}}{S} \sum_x \text{tr}_{\text{rest}}(M_j^l(x, t)),$$

where

$$M_j^l = \left[ U_j^l \dots U_1^1 (|\psi_x^{\text{in}}\rangle \langle \psi_x^{\text{in}}| \otimes |0\dots 0\rangle \langle 0\dots 0|) U_1^{1\dagger} \dots U_j^{l\dagger}, \right. \\ \left. U_{j+1}^{l\dagger} \dots U_{m_{L+1}}^{L+1\dagger} (\mathbb{1}_{\text{in+hid}} \otimes |1\rangle \langle 1|) U_{m_{L+1}}^{L+1} \dots U_{l+1}^l \right]$$

for  $l \leq g$  and

$$M_j^l = \left[ U_j^l \dots U_1^{g+1} |\phi^T\rangle \langle \phi^T| \otimes |0\dots 0\rangle \langle 0\dots 0| U_1^{g+1\dagger} \dots U_j^{l\dagger} \right. \\ \left. - U_j^l \dots U_1^{g+1} U_{m_g}^g \dots U_1^1 (|\psi_x^{\text{in}}\rangle \langle \psi_x^{\text{in}}| \otimes |0\dots 0\rangle \langle 0\dots 0|) U_1^{1\dagger} \dots U_{m_g}^{g\dagger} U_1^{g+1\dagger} \dots U_j^{l\dagger}, \right. \\ \left. U_{j+1}^{l\dagger} \dots U_{m_{L+1}}^{L+1\dagger} (\mathbb{1}_{\text{in+hid}} \otimes |1\rangle \langle 1|) U_{m_{L+1}}^{L+1} \dots U_{l+1}^l \right]$$

else. Here,  $U_j^l$  is assigned to the  $j$ th perceptron acting on layers  $l-1$  and  $l$ ,  $g$  is the number of perceptron layers of the generator, and  $\eta$  is the learning rate.

The proof can be found in Appendix A. Note, that in the following only DQGANs of three layers are used, i.e. both DQNNs are built of two qubit layers connected by one

perceptron layer, respectively. Hence, we assume  $g = 1$  in the following.

In analogy to training the DQNN<sub>Q</sub>, the implementation on a quantum computer is done via parameterised quantum gates, which are updated using gradient descent. The training losses  $\mathcal{L}_G$  and  $\mathcal{L}_D$  are evaluated via measurement of the discriminator’s output qubit.

At the end of the training the goal is that every generator output is close to at least one of the given states  $\{|\phi_x^T\rangle\}_{x=1}^N$ . To test this we additionally generate  $V$  random states  $|\psi^{\text{in}}\rangle$  as input states of the generator. We refer to the corresponding generated states as validation states. For each validation state, we search for the closest state of the data set via  $\max_{x=1}^N (\langle\phi_x^T|\mathcal{E}_G(|\psi_i^{\text{in}}\rangle\langle\psi_i^{\text{in}}|)|\phi_x^T\rangle)$ . Using all validation states we define the *validation loss*

$$\mathcal{L}_V(\mathcal{E}_G) = \frac{1}{V} \sum_{i=1}^V \max_{x=1}^N (\langle\phi_x^T|\mathcal{E}_G(|\psi_i^{\text{in}}\rangle\langle\psi_i^{\text{in}}|)|\phi_x^T\rangle).$$

Note that the above-defined validation loss would be optimised indeed if the generator produces only a small variety of states or even exactly one state. As long as these are close to at least one of the training states, the validation loss is high. Therefore, it is important to check the diversity of the generator’s output, which will be described in Section 4.

### 3 Results

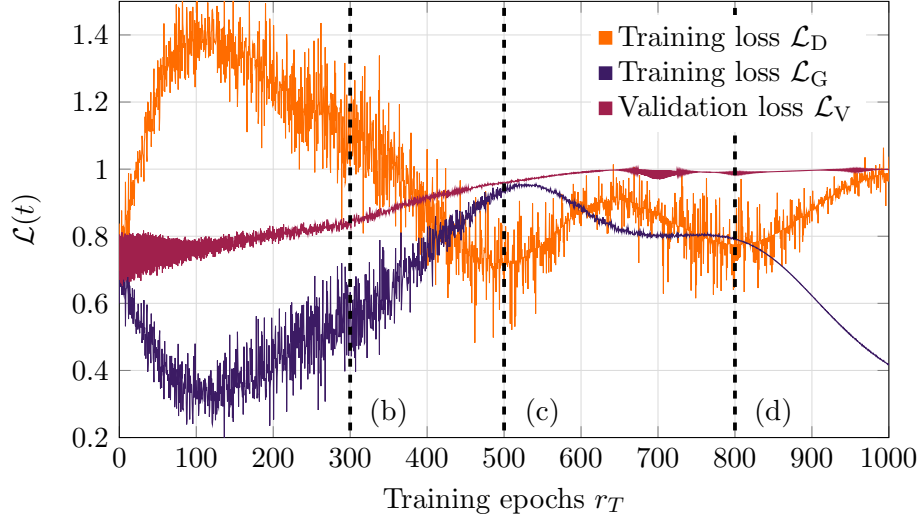
In the following we test the training algorithm including the two training functions  $\mathcal{L}_G$  and  $\mathcal{L}_D$ . Here, we use the simulation on a classical computer. The code can be found at [61]. As the training data we prepare a set of pure one-qubit states which build a line on the Bloch sphere, namely

$$\text{data}_{\text{line}} = \left\{ \frac{(N-x)|0\rangle + (x-1)|1\rangle}{\|(N-x)|0\rangle + (x-1)|1\rangle\|} \right\}_{x=1}^N,$$

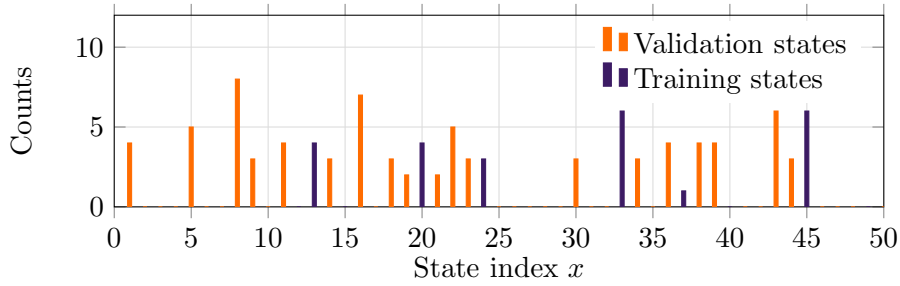
for  $N = 50$ . Next, we randomly shuffle this set of states. The first  $S$  of the resulting set  $\{|\psi_x^T\rangle\}_{x=1}^S$  will be used for the training process. The full data set  $\{|\psi_x^T\rangle\}_{x=1}^N$  is used for computing the validation loss.

In Fig. 3a the evolution of the discriminator’s and generator’s training losses and the validation loss is plotted. The latter reaches values over 0.95 at  $t = 9.5$ , i.e., after training round  $r_T = 475$ . Moreover, we can observe that in the first training epochs, the training loss of the generator shrinks and the discriminator training loss increases. This behaviour inverts at  $t \approx 2$ . For the remaining training process, this switch between an increasing generator training loss and an increasing discriminator training loss happens repetitively. We explain this behaviour with the opposing goals of the generator and the discriminator and a changing dominance of one of the networks.

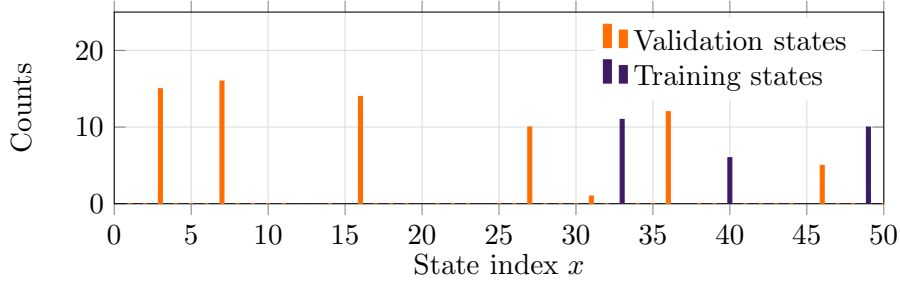
The saturating validation loss in Fig. 3a gives the impression that the longer we train the DQGAN, the better the results. In the original proposal of the DQNN [18] this was the case. However, the validation loss would be maximal if the generator would



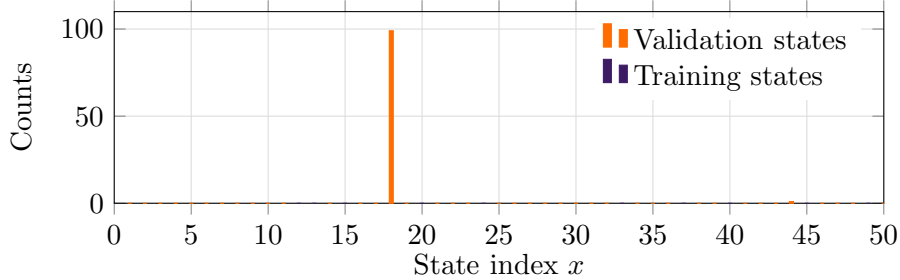
(a) Loss functions.



(b) Diversity of the generator's output ater  $r_T = 300$  training epochs.



(c) Diversity of the generator's output ater  $r_T = 500$  training epochs.

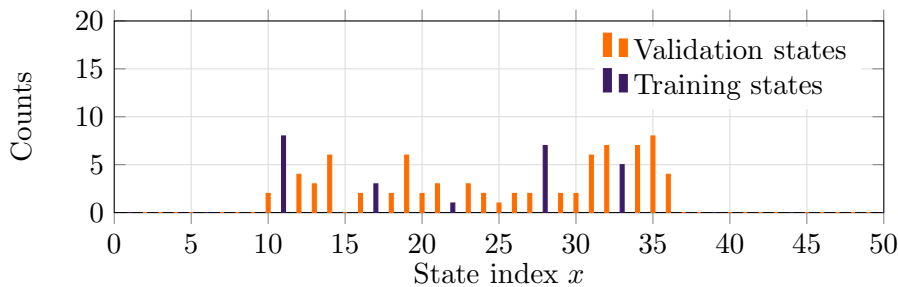


(d) Diversity of the generator's output ater  $r_T = 800$  training epochs.

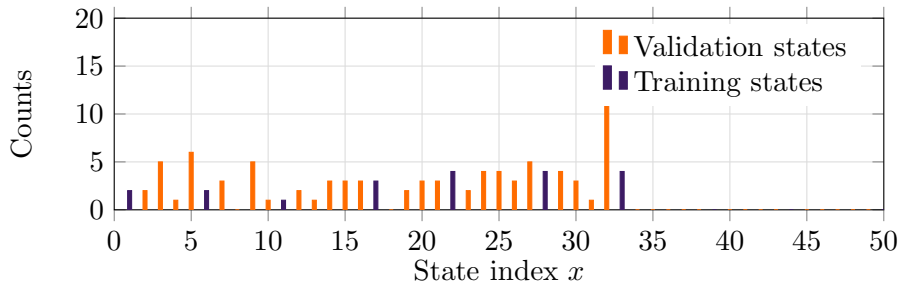
Figure 3: **Training a DQGAN.** (a) depicts the evolution of the loss functions during the training of a  $\circ-\circ-\circ$  DQGAN in  $r_T = 1000$  epochs with  $\eta = 1$  and  $\epsilon = 0.01$  using 50 data pairs where 10 are used as training states. The dashed lines mark the diversity checks 300 (b), 500 (c) and 800 (d) for the generator's output.

permanently produce the exact same state when this state is one of the training states  $\{|\psi_x^T\rangle\}_{x=1}^N$ . This would not fit our aim to train the generator to extended the training set. Hence, we explain in the following how we check the *diversity* of the generator’s output.

After training for  $r_T$  rounds, we use the generator to produce a set of 100 states. Using the fidelity, we find for each of these states the element of  $\text{data}_{\text{line}}$ , which is the closest. In this way, we obtain a number for every index  $x$  of this set describing how often the output of the generator was most closely to the  $x$ th element of  $\text{data}_{\text{line}}$ . In Fig. 3b to 3d we plot these numbers in the form of an histogram. The different colours describe whether an element of  $\text{data}_{\text{line}}$  was used as a training state or not. We find that the diversity was good after 300 training epochs. However, it decreases afterwards in the ongoing training. We point to Appendix C for more numerical results.



(a) Diversity of the generator’s output after  $r_T = 100$  training epochs.



(b) Diversity of the generator’s output after  $r_T = 440$  training epochs.

Figure 4: **Training a DQGAN<sub>Q</sub>**. The training set features  $S = 10$  equally spaced quantum states from  $\text{data}_{\text{line}}$ . The remaining states from  $\text{data}_{\text{line}}$  are used as validation states. The DQGAN<sub>Q</sub> features a 1-1<sup>+</sup> generator DQNN<sub>Q</sub> and a 1-1<sup>+</sup> discriminator DQNN<sub>Q</sub>, and employs the hyper-parameters  $r_D = 4$ ,  $\eta_D = 0.5$ ,  $r_G = 1$  and  $\eta_G = 0.1$ .

In addition to the DQGAN simulation on a classical computer we also simulate the DQGAN<sub>Q</sub> under noiseless circumstances. Here, the same training loss functions  $\mathcal{L}_G, \mathcal{L}_D$  are used as well as the same training data,  $\text{data}_{\text{line}}$ . In this case, the training states are not picked randomly but  $S = 10$  equally spaced training states are chosen from  $\text{data}_{\text{line}}$ . The hyper-parameters of the training are chosen such that for each of the  $r_T$  epochs, a

1-1<sup>+</sup> discriminator  $\text{DQNN}_Q$  is trained  $r_D = 4$  times with a learning rate  $\eta_D = 0.5$  and a 1-1<sup>+</sup> generator is trained  $r_G = 1$  times with a learning rate  $\eta_G = 0.1$ . The + denotes a slightly different implementation of  $\text{DQGAN}_Q$  compared to implementation discussed in [17]. It uses additional gates and is explained in Algorithm 1.

The results of training the  $\text{DQGAN}_Q$  are shown in are shown in Fig. 4. The generator’s diversity after training for  $r_T = 100$  epochs is depicted in Fig. 4a. Here, the generator achieves to produce states in a little more than half of the training data range. After  $r_T = 440$  training epochs, the generator’s diversity is improved to two-thirds of the training data range as depicted in Fig. 4b. Please note that in both cases, the majority of the generator’s produced states is closer to a validation state than a training state. This can be seen as a training success as the generator does not only learn to reproduce the training states but instead learns to extend the given training data.

For more numerical results using  $\text{DQGAN}_Q$  we point to Appendix C and [74].

## 4 Discussion

In this work, we introduced  $\text{DQGANs}$ , generative adversarial models based on the  $\text{DQNN}$  proposed in [18]. A  $\text{DQGAN}$  features two  $\text{DQNNs}$  trained in an opposing manner: the discriminator’s goal is to distinguish between synthetic, by the generator produced quantum states and elements of the training data set. On the contrary, the generator aims to produce data with similar properties as the states included in the training data set.

We aimed to extend a given data set with states with similar characteristics. Our examples have shown that this goal can be reached when training a  $\text{DQGAN}$ . However, due to limitations in computational power, we could only train small  $\text{DQGAN}$  architectures and therefore leave questions open for future research. It would be interesting if using larger  $\text{DQNNs}$  for the generator or the discriminator leads to better validation loss values or more diversity in the generator’s output. Further, the study of other data sets is of interest. One example could be a set of states with similar degrees of entanglement (with respect to a chosen entanglement measure) [75]. Since in classical machine learning, the output of  $\text{GANs}$  is often used to train other neural network architectures, a similar application for  $\text{DQGANs}$  and  $\text{DQNNs}$  is conceivable.

**Acknowledgements** The authors would like to thank Tobias J. Osborne and Christian Struckmann for valuable discussions. Moreover, helpful correspondence with Dmytro Bondarenko, Terry Farrelly, Polina Feldmann, Daniel List, Jan Hendrik Pfau, Robert Salzmann, Daniel Scheiermann, Viktoria Schmiesing, Marvin Schwiering, and Ramona Wolf is gratefully acknowledged. This work was supported, in part, by the DFG through SFB 1227 (DQ-mat), Quantum Valley Lower Saxony, and funded by the Deutsche Forschungsgemeinschaft (DFG, German Research Foundation) under Germanys Excellence Strategy EXC-2123 QuantumFrontiers 390837967.

## References

- [1] J. Preskill. Quantum computing in the NISQ era and beyond. *Quantum*, 2:79, 2018. doi:10.22331/q-2018-08-06-79.
- [2] M. Brooks. Beyond quantum supremacy: the hunt for useful quantum computers. *Nature*, 574(7776):19–21, 2019. doi:10.1038/d41586-019-02936-3.
- [3] F. Arute, K. Arya, R. Babbush, D. Bacon, J. C. Bardin, R. Barends, R. Biswas, S. Boixo, F. G. S. L. Brandao, D. A. Buell, B. Burkett, Y. Chen, Z. Chen, B. Chiaro, R. Collins, W. Courtney, A. Dunsworth, E. Farhi, B. Foxen, A. Fowler, C. Gidney, M. Giustina, R. Graff, K. Guerin, S. Habegger, M. P. Harrigan, M. J. Hartmann, A. Ho, M. Hoffmann, T. Huang, T. S. Humble, S. V. Isakov, E. Jeffrey, Z. Jiang, D. Kafri, K. Kechedzhi, J. Kelly, P. V. Klimov, S. Knysh, A. Korotkov, F. Kostritsa, D. Landhuis, M. Lindmark, E. Lucero, D. Lyakh, S. Mandrà, J. R. McClean, M. McEwen, A. Megrant, X. Mi, K. Michielsen, M. Mohseni, J. Mutus, O. Naaman, M. Neeley, C. Neill, M. Y. Niu, E. Ostby, A. Petukhov, J. C. Platt, C. Quintana, E. G. Rieffel, P. Roushan, N. C. Rubin, D. Sank, K. J. Satzinger, V. Smelyanskiy, K. J. Sung, M. D. Trevithick, A. Vainsencher, B. Villalonga, T. White, Z. J. Yao, P. Yeh, A. Zalcman, H. Neven, and J. M. Martinis. Quantum supremacy using a programmable superconducting processor. *Nature*, 574(7779):505–510, 2019. doi:10.1038/s41586-019-1666-5.
- [4] P. Shor. Fault-tolerant quantum computation. In *Proceedings of 37th Conference on Foundations of Computer Science*, pages 56–65, 1996. doi:10.1109/SFCS.1996.548464.
- [5] J. Preskill. Fault-tolerant quantum computation. In *Introduction to quantum computation and information*, pages 213–269. World Scientific, 1998. doi:10.1142/9789812385253\_0008.
- [6] M. A. Nielsen and I. L. Chuang. *Quantum Computation and Quantum Information*. Cambridge University Press, 2000.
- [7] P. Shor. Algorithms for quantum computation: discrete logarithms and factoring. In *Proceedings 35th Annual Symposium on Foundations of Computer Science*, pages 124–134, 1994. doi:10.1109/SFCS.1994.365700.
- [8] S. Lloyd. Universal quantum simulators. *Science*, 273(5278):1073–1078, 1996.
- [9] M. Cerezo, A. Arrasmith, R. Babbush, S. C. Benjamin, S. Endo, K. Fujii, J. R. McClean, K. Mitarai, X. Yuan, L. Cincio, et al. Variational quantum algorithms. 2020, arXiv:2012.09265.
- [10] K. Mitarai, M. Negoro, M. Kitagawa, and K. Fujii. Quantum circuit learning. *Physical Review A*, 2018. doi:10.1103/PhysRevA.98.032309.

- [11] J. Stokes, J. Izaac, N. Killoran, and G. Carleo. Quantum Natural Gradient. *Quantum*, 2020. doi:10.22331/q-2020-05-25-269.
- [12] M. Schuld, V. Bergholm, C. Gogolin, J. Izaac, and N. Killoran. Evaluating analytic gradients on quantum hardware. 99(3):032331. doi:10.1103/PhysRevA.99.032331.
- [13] M. Ostaszewski, E. Grant, and M. Benedetti. Quantum circuit structure learning. 2019, arXiv:1905.09692.
- [14] K. Bu, D. E. Koh, L. Li, Q. Luo, and Y. Zhang. On the statistical complexity of quantum circuits. 2021, arXiv:2101.06154.
- [15] M. Benedetti, E. Lloyd, S. Sack, and M. Fiorentini. Parameterized quantum circuits as machine learning models. *Quantum Science and Technology*, 4(4):043001, 2019. doi:10.1088/2058-9565/ab5944.
- [16] Y. Du, M.-H. Hsieh, T. Liu, and D. Tao. The Expressive Power of Parameterized Quantum Circuits. 2018, arXiv:1810.11922.
- [17] K. Beer, D. List, G. Müller, T. J. Osborne, and C. Struckmann. Training Quantum Neural Networks on NISQ Devices. 2021, arXiv:2104.06081.
- [18] K. Beer, D. Bondarenko, T. Farrelly, T. J. Osborne, R. Salzmann, D. Scheiermann, and R. Wolf. Training deep quantum neural networks. *Nature Communications*, 11(1):1–6, 2020. doi:10.1038/s41467-020-14454-2.
- [19] D. Bondarenko and P. Feldmann. Quantum Autoencoders to Denoise Quantum Data. *Physical Review Letters*, 124:130502, 2020. doi:10.1103/PhysRevLett.124.130502.
- [20] K. Beer, M. Khosla, J. Köhler, and T. J. Osborne. Quantum machine learning of graph-structured data. 2021, arXiv:2103.10837.
- [21] M. Schuld and N. Killoran. Quantum machine learning in feature Hilbert spaces. *Physical Review Letters*, 122(4):040504, 2019. doi:10.1103/PhysRevLett.122.040504.
- [22] M. Schuld, A. Bocharov, K. M. Svore, and N. Wiebe. Circuit-centric quantum classifiers. *Physical Review A*, 101(3):032308, 2020. doi:10.1103/PhysRevA.101.032308.
- [23] K. Zhang, M.-H. Hsieh, L. Liu, and D. Tao. Toward trainability of quantum neural networks. 2020, arXiv:2011.06258.
- [24] T. Achache, L. Horesh, and J. Smolin. Denoising quantum states with Quantum Autoencoders—Theory and Applications. 2020, arXiv:2012.14714.
- [25] K. H. Wan, O. Dahlsten, H. Kristjánsson, R. Gardner, and M. Kim. Quantum generalisation of feedforward neural networks. *npj Quantum Information*, 3(1):1–8, 2017. doi:10.1038/s41534-017-0032-4.

- [26] J. Romero, J. P. Olson, and A. Aspuru-Guzik. Quantum autoencoders for efficient compression of quantum data. *Quantum Science and Technology*, 2(4):045001, 2017. doi:<https://doi.org/10.1088/2058-9565/aa8072>.
- [27] A. Pepper, N. Tischler, and G. J. Pryde. Experimental realization of a quantum autoencoder: The compression of qutrits via machine learning. *Physical review letters*, 122(6):060501, 2019. doi:[10.1103/PhysRevLett.122.060501](https://doi.org/10.1103/PhysRevLett.122.060501).
- [28] B. T. Kiani, S. Lloyd, and R. Maity. Learning unitaries by gradient descent. 2020, [arXiv:2001.11897](https://arxiv.org/abs/2001.11897).
- [29] M. R. Geller, Z. Holmes, P. J. Coles, and A. Sornborger. Experimental Quantum Learning of a Spectral Decomposition. 2021, [arXiv:2104.03295](https://arxiv.org/abs/2104.03295).
- [30] G. Verdon, J. Pye, and M. Broughton. A Universal Training Algorithm for Quantum Deep Learning. 2018, [arXiv:1806.09729](https://arxiv.org/abs/1806.09729).
- [31] M. Sedláč, A. Bisio, and M. Ziman. Optimal probabilistic storage and retrieval of unitary channels. *Physical Review Letters*, 2019. doi:[10.1103/PhysRevLett.122.170502](https://doi.org/10.1103/PhysRevLett.122.170502).
- [32] G. Verdon, T. McCourt, E. Luzhnica, V. Singh, S. Leichenauer, and J. Hidary. Quantum Graph Neural Networks. 2019, [arXiv:1909.12264](https://arxiv.org/abs/1909.12264).
- [33] I. Cong, S. Choi, and M. D. Lukin. Quantum convolutional neural networks. *Nature Physics*, 15(12):1273–1278, 2019. doi:[10.1038/s41567-019-0648-8](https://doi.org/10.1038/s41567-019-0648-8).
- [34] S. Arunachalam and R. de Wolf. A Survey of Quantum Learning Theory. 2017, [arXiv:1701.06806](https://arxiv.org/abs/1701.06806).
- [35] I. Goodfellow, J. Pouget-Abadie, M. Mirza, B. Xu, D. Warde-Farley, S. Ozair, A. Courville, and Y. Bengio. Generative adversarial nets. 2014, [arXiv:1602.04799](https://arxiv.org/abs/1602.04799).
- [36] P.-L. Dallaire-Demers and N. Killoran. Quantum generative adversarial networks. *Phys. Rev. A*, 2018. doi:[10.1103/PhysRevA.98.012324](https://doi.org/10.1103/PhysRevA.98.012324).
- [37] M. Y. Niu, A. Zlokapa, M. Broughton, S. Boixo, M. Mohseni, V. Smelyanskiy, and H. Neven. Entangling Quantum Generative Adversarial Networks. [arXiv:2105.00080](https://arxiv.org/abs/2105.00080). doi:[2021](https://doi.org/10.26434/chemrxiv-2021-00080).
- [38] S. Lloyd and C. Weedbrook. Quantum Generative Adversarial Learning. *Phys. Rev. Lett.*, 2018. doi:[10.1103/PhysRevLett.121.040502](https://doi.org/10.1103/PhysRevLett.121.040502).
- [39] M. Benedetti, E. Grant, L. Wossnig, and S. Severini. Adversarial quantum circuit learning for pure state approximation. *New Journal of Physics*, 2019. doi:[10.1088/1367-2630/ab14b5](https://doi.org/10.1088/1367-2630/ab14b5).
- [40] S. Chakrabarti, Y. Huang, T. Li, S. Feizi, and X. Wu. Quantum wasserstein generative adversarial networks. 2019, [arXiv:1911.00111](https://arxiv.org/abs/1911.00111).

- [41] L. Hu, S.-H. Wu, W. Cai, Y. Ma, X. Mu, Y. Xu, H. Wang, Y. Song, D.-L. Deng, C.-L. Zou, and L. Sun. Quantum generative adversarial learning in a superconducting quantum circuit. *Science Advances*, 5(1):10, 2019. doi:10.1126/sciadv.aav2761.
- [42] C. Zoufal, A. Lucchi, and S. Woerner. Quantum generative adversarial networks for learning and loading random distributions. *npj Quantum Information*, 5(1):103. doi:10.1038/s41534-019-0223-2.
- [43] C. Zoufal. *Generative Quantum Machine Learning*. PhD thesis, 2021, arXiv:2111.12738.
- [44] S. A. Stein, B. Baheri, D. Chen, Y. Mao, Q. Guan, A. Li, B. Fang, and S. Xu. QuGAN: A Quantum State Fidelity based Generative Adversarial Network. In *2021 IEEE International Conference on Quantum Computing and Engineering (QCE)*, pages 71–81. doi:10.1109/QCE52317.2021.00023.
- [45] K. Huang, Z.-A. Wang, C. Song, K. Xu, H. Li, Z. Wang, Q. Guo, Z. Song, Z.-B. Liu, D. Zheng, D.-L. Deng, H. Wang, J.-G. Tian, and H. Fan. Quantum generative adversarial networks with multiple superconducting qubits. 7(1). doi:10.1038/s41534-021-00503-1.
- [46] M. Andrecut and M. Ali. A quantum neural network model. *International Journal of Modern Physics C*, 13(01):75–88, 2002. doi:10.1142/S0129183102002948.
- [47] W. R. d. Oliveira, A. J. Silva, T. B. Ludermir, A. Leonel, W. R. Galindo, and J. C. Pereira. Quantum logical neural networks. In *10th Brazilian Symposium on Neural Networks*, pages 147–152, 2008. doi:10.1109/SBRN.2008.9.
- [48] M. Panella and G. Martinelli. Neural networks with quantum architecture and quantum learning. *International Journal of Circuit Theory and Applications*, 39(1):61–77, 2011. doi:10.1002/cta.619.
- [49] A. J. da Silva, T. B. Ludermir, and W. R. de Oliveira. Quantum perceptron over a field and neural network architecture selection in a quantum computer. 76:55–64, 2016. doi:10.1016/j.neunet.2016.01.002.
- [50] Y. Cao, G. G. Guerreschi, and A. Aspuru-Guzik. Quantum Neuron: an elementary building block for machine learning on quantum computers. arXiv:1711.11240.
- [51] U. Alvarez-Rodriguez, L. Lamata, P. Escandell-Montero, J. D. Martín-Guerrero, and E. Solano. Supervised quantum learning without measurements. *Scientific reports*, 7(1):1–9, 2017. doi:10.1038/s41598-017-13378-0.
- [52] E. Farhi and H. Neven. Classification with Quantum Neural Networks on Near Term Processors. 2018, arXiv:1802.06002.
- [53] N. Killoran, T. R. Bromley, J. M. Arrazola, M. Schuld, N. Quesada, and S. Lloyd. Continuous-variable quantum neural networks. *Phys. Rev. Research*, 2019. doi:10.1103/PhysRevResearch.1.033063.

- [54] G. R. Steinbrecher, J. P. Olson, D. Englund, and J. Carolan. Quantum optical neural networks. *npj Quantum Information*, 5(1):1–9, 2019. doi:10.1038/s41534-019-0174-7.
- [55] E. Torrontegui and J. J. García-Ripoll. Unitary quantum perceptron as efficient universal approximator. *EPL (Europhysics Letters)*, 125(3):30004, 2019. doi:10.1209/0295-5075/125/30004.
- [56] G. Sentís, A. Monràs, R. Muñoz Tapia, J. Calsamiglia, and E. Bagan. Unsupervised Classification of Quantum Data. *Phys. Rev. X*, 2019. doi:10.1103/PhysRevX.9.041029.
- [57] F. Tacchino, P. Barkoutsos, C. Macchiavello, I. Tavernelli, D. Gerace, and D. Bajoni. Quantum implementation of an artificial feed-forward neural network. *Quantum Science and Technology*, 5(4):044010, 2020. doi:10.1088/2058-9565/abb8e4.
- [58] A. Skolik, J. R. McClean, M. Mohseni, P. van der Smagt, and M. Leib. Layerwise learning for quantum neural networks. 2020, arXiv:2006.14904.
- [59] K. Sharma, M. Cerezo, L. Cincio, and P. J. Coles. Trainability of Dissipative Perceptron-Based Quantum Neural Networks. 2020, arXiv:2005.12458.
- [60] Y. Zhang and Q. Ni. Design of quantum neuron model for quantum neural networks. *Quantum Engineering*, 3(3):e75, 2021. doi:10.1002/que2.75.
- [61] Dissipative quantum neural networks - Python Code. URL <https://github.com/qigitphannover/DeepQuantumNeuralNetworks>.
- [62] J. Zhang, J. Vala, S. Sastry, and K. B. Whaley. Geometric theory of nonlocal two-qubit operations. *Physical Review A*, 67(4):042313, 2003. doi:10.1103/PhysRevA.67.042313.
- [63] J. Zhang, J. Vala, S. Sastry, and K. B. Whaley. Optimal quantum circuit synthesis from controlled-unitary gates. *Physical Review A*, 69(4):042309, 2004. doi:10.1103/PhysRevA.69.042309.
- [64] M. Blaauboer and R. De Visser. An analytical decomposition protocol for optimal implementation of two-qubit entangling gates. *Journal of Physics A: Mathematical and Theoretical*, 41(39):395307, 2008. doi:10.1088/1751-8113/41/39/395307.
- [65] P. Watts, M. O’Connor, and J. Vala. Metric structure of the space of two-qubit gates, perfect entanglers and quantum control. *Entropy*, 15(6):1963–1984, 2013. doi:10.3390/e15061963.
- [66] G. E. Crooks. Gradients of parameterized quantum gates using the parameter-shift rule and gate decomposition. 2019, arXiv:1905.13311.
- [67] E. C. Peterson, G. E. Crooks, and R. S. Smith. Two-qubit circuit depth and the monodromy polytope. *Quantum*, 4:247, 2020. doi:10.22331/q-2020-03-26-247.

- [68] M. A. Nielsen. *Neural networks and deep learning*, volume 25. Determination press San Francisco, CA, 2015.
- [69] A. Creswell, T. White, V. Dumoulin, K. Arulkumaran, B. Sengupta, and A. A. Bharath. Generative adversarial networks: An overview. *IEEE Signal Processing Magazine*, 35(1):53–65, 2018. doi:10.1109/MSP.2017.2765202.
- [70] J.-Y. Zhu, P. Krähenbühl, E. Shechtman, and A. A. Efros. Generative visual manipulation on the natural image manifold. In *European conference on computer vision*, pages 597–613. Springer, 2016. doi:10.1007/978-3-319-46454-1\_36.
- [71] T. Salimans, I. Goodfellow, W. Zaremba, V. Cheung, A. Radford, and X. Chen. Improved Techniques for Training GANs. *Advances in neural information processing systems*, 29:2234–2242, 2016.
- [72] S. Reed, Z. Akata, X. Yan, L. Logeswaran, B. Schiele, and H. Lee. Generative adversarial text to image synthesis. In M. F. Balcan and K. Q. Weinberger, editors, *Proceedings of The 33rd International Conference on Machine Learning*, volume 48, pages 1060–1069, 2016.
- [73] C. Ledig, L. Theis, F. Huszár, J. Caballero, A. Cunningham, A. Acosta, A. Aitken, A. Tejani, J. Totz, Z. Wang, et al. Photo-realistic single image super-resolution using a generative adversarial network. In *Proceedings of the IEEE conference on computer vision and pattern recognition*, pages 4681–4690, 2017.
- [74] G. Müller, Generative Adversarial Learning with Quantum Neural Networks. Master’s thesis, 2021.
- [75] L. Schatzki, A. Arrasmith, P. J. Coles, and M. Cerezo. Entangled datasets for quantum machine learning. 2021, arXiv:2109.03400v2.

## A Derivation of the update matrices

Analogously to the DQNN update rule presented in [18] the unitaries will be updated through

$$U_j^l(t + \epsilon) = e^{i\epsilon K_j^l(t)} U_j^l(t).$$

We will derive the update matrices in general in Proposition 1. To understand the basic idea we discuss the update of a DQGAN consisting of three unitaries, see Fig. 2, first. These perceptron unitaries have the following update rules:

$$\begin{aligned} U_D(t + \epsilon) &= e^{i\epsilon K_D(t)} U_D(t) \\ U_{G1}(t + \epsilon) &= e^{i\epsilon K_{G1}(t)} U_{G1}(t) \\ U_{G2}(t + \epsilon) &= e^{i\epsilon K_{G2}(t)} U_{G2}(t). \end{aligned}$$

Note that the unitaries act on the current layers, e.g.  $U_{G1}$  denotes  $U_{G1} \otimes \mathbb{1}$  and  $U_{G2}$  denotes  $\mathbb{1} \otimes U_{G2}$ .

In the first part of the algorithm the generator is fixed and only the discriminator is updated. When the training data is the discriminator's input we get the output state

$$\begin{aligned} \rho_{\text{out}}^D(t + \epsilon) &= \text{tr}_{\{2,3\}} \left( e^{i\epsilon K_D} U_D |\phi^T\rangle \langle \phi^T| \otimes |0\rangle \langle 0| U_D^\dagger e^{-i\epsilon K_D} \right) \\ &= \text{tr}_{\{2,3\}} \left( U_D |\phi^T\rangle \langle \phi^T| \otimes |0\rangle \langle 0| U_D^\dagger + i\epsilon \left[ K_D, U_D |\phi^T\rangle \langle \phi^T| \otimes |0\rangle \langle 0| U_D^\dagger \right] \right. \\ &\quad \left. + \mathcal{O}(\epsilon^2) \right) \\ &= \rho_{\text{out}}^D(t) + i\epsilon \text{tr}_{\{2,3\}} \left( \left[ K_D, U_D |\phi^T\rangle \langle \phi^T| \otimes |0\rangle \langle 0| U_D^\dagger \right] \right) + \mathcal{O}(\epsilon^2). \end{aligned}$$

If the discriminator gets the generator's output as input we get the output state

$$\begin{aligned} \rho_{\text{out}}^{G+D}(t + \epsilon) &= \text{tr}_{\{1,2,3\}} \left( e^{i\epsilon K_D} U_D U_{G2} U_{G1} (|\psi_x^{\text{in}}\rangle \langle \psi_x^{\text{in}}| \otimes |000\rangle \langle 000|) U_{G1}^\dagger U_{G2}^\dagger U_D^\dagger e^{-i\epsilon K_D} \right) \\ &= \text{tr}_{\{1,2,3\}} \left( U_D U_{G2} U_{G1} (|\psi_x^{\text{in}}\rangle \langle \psi_x^{\text{in}}| \otimes |000\rangle \langle 000|) U_{G1}^\dagger U_{G2}^\dagger U_D^\dagger \right. \\ &\quad \left. + i\epsilon \left[ K_D, U_D U_{G2} U_{G1} (|\psi_x^{\text{in}}\rangle \langle \psi_x^{\text{in}}| \otimes |000\rangle \langle 000|) U_{G1}^\dagger U_{G2}^\dagger U_D^\dagger \right] + \mathcal{O}(\epsilon^2) \right) \\ &= \rho_{\text{out}}^{G+D}(t) \\ &\quad + i\epsilon \text{tr}_{\{1,2,3\}} \left( \left[ K_D, U_D U_{G2} U_{G1} (|\psi_x^{\text{in}}\rangle \langle \psi_x^{\text{in}}| \otimes |000\rangle \langle 000|) U_{G1}^\dagger U_{G2}^\dagger U_D^\dagger \right] \right) \\ &\quad + \mathcal{O}(\epsilon^2). \end{aligned}$$

The update of the generator, assuming the discriminator is fixed, can be written as

$$\begin{aligned} \rho_{\text{out}2}^{G+D}(t + \epsilon) &= \text{tr}_{\{1,2,3\}} \left( U_D e^{i\epsilon K_{G2}} U_{G2} e^{i\epsilon K_{G1}} U_{G1} (|\psi_x^{\text{in}}\rangle \langle \psi_x^{\text{in}}| \otimes |000\rangle \langle 000|) \right. \\ &\quad \left. U_{G1}^\dagger e^{-i\epsilon K_{G1}} U_{G2}^\dagger e^{-i\epsilon K_{G2}} U_D^\dagger \right) \end{aligned}$$

$$\begin{aligned}
&= \text{tr}_{\{1,2,3\}} \left( U_D \left( U_{G2} U_{G1} (|\psi_x^{\text{in}}\rangle \langle \psi_x^{\text{in}}| \otimes |000\rangle \langle 000|) U_{G1}^\dagger U_{G2}^\dagger \right. \right. \\
&\quad + i\epsilon U_{G2} \left[ K_{G1}, U_{G1} (|\psi_x^{\text{in}}\rangle \langle \psi_x^{\text{in}}| \otimes |000\rangle \langle 000|) U_{G1}^\dagger \right] U_{G2}^\dagger \\
&\quad \left. \left. + i\epsilon \left[ K_{G2}, U_{G2} U_{G1} (|\psi_x^{\text{in}}\rangle \langle \psi_x^{\text{in}}| \otimes |000\rangle \langle 000|) U_{G1}^\dagger U_{G2}^\dagger \right] \right) U_D^\dagger + \mathcal{O}(\epsilon^2) \right) \\
&= \rho_{\text{out}2}^{G+D}(t) \\
&\quad + i\epsilon \text{tr}_{\{1,2,3\}} \left( U_D \left( U_{G2} \left[ K_{G1}, U_{G1} (|\psi_x^{\text{in}}\rangle \langle \psi_x^{\text{in}}| \otimes |000\rangle \langle 000|) U_{G1}^\dagger \right] U_{G2}^\dagger \right. \right. \\
&\quad \left. \left. + \left[ K_{G2}, U_{G2} U_{G1} (|\psi_x^{\text{in}}\rangle \langle \psi_x^{\text{in}}| \otimes |000\rangle \langle 000|) U_{G1}^\dagger U_{G2}^\dagger \right] \right) U_D^\dagger \right) + \mathcal{O}(\epsilon^2).
\end{aligned}$$

To derive the update matrices in general we assume in the following a generator consisting of unitaries  $U_1^1 \dots U_{m_g}^g$  and a discriminator built of unitaries  $U_1^{g+1} \dots U_{m_{L+1}}^{L+1}$ . The update matrices  $K_j^l$  update the generator, if  $l \leq g$  for the number of perceptron layers  $g$  of the generator. Otherwise, the matrices  $K_j^l$  describe discriminator updates.

**Proposition 1.** *The update matrix for a QGAN trained with pure states  $|\phi_x^T\rangle$  has to be of the form*

$$K_j^l(t) = \frac{\eta 2^{m_l-1} i}{S} \sum_x \text{tr}_{\text{rest}} (M_j^l(x, t)),$$

where

$$\begin{aligned}
M_j^l &= \left[ U_j^l \dots U_1^1 (|\psi_x^{\text{in}}\rangle \langle \psi_x^{\text{in}}| \otimes |0\dots 0\rangle \langle 0\dots 0|) U_1^{1\dagger} \dots U_j^{l\dagger}, \right. \\
&\quad \left. U_{j+1}^{l\dagger} \dots U_{m_{L+1}}^{L+1\dagger} (\mathbb{1}_{\text{in+hid}} \otimes |1\rangle \langle 1|) U_{m_{L+1}}^{L+1} \dots U_{l+1}^l \right]
\end{aligned}$$

for  $l \leq g$  and

$$\begin{aligned}
M_j^l &= \left[ U_j^l \dots U_1^{g+1} (|\phi^T\rangle \langle \phi^T| \otimes |0\dots 0\rangle \langle 0\dots 0|) U_1^{g+1\dagger} \dots U_j^{l\dagger} \right. \\
&\quad \left. - U_j^l \dots U_1^{g+1} U_{m_g}^g \dots U_1^1 (|\psi_x^{\text{in}}\rangle \langle \psi_x^{\text{in}}| \otimes |0\dots 0\rangle \langle 0\dots 0|) U_1^{1\dagger} \dots U_{m_g}^{g\dagger} U_1^{g+1\dagger} \dots U_j^{l\dagger}, \right. \\
&\quad \left. U_{j+1}^{l\dagger} \dots U_{m_{L+1}}^{L+1\dagger} (\mathbb{1}_{\text{in+hid}} \otimes |1\rangle \langle 1|) U_{m_{L+1}}^{L+1} \dots U_{l+1}^l \right]
\end{aligned}$$

Here,  $U_j^l$  is assigned to the  $j$ th perceptron acting on layers  $l-1$  and  $l$ ,  $g$  is the number of perceptron layers of the generator, and  $\eta$  is the learning rate.

*Proof.* First, we compute the output state of the discriminator after an update with  $K_D$ . Note that in the following the unitaries act on the current layers, e.g.  $U_1^l$  denotes actually  $U_1^l \otimes \mathbb{1}_{2,3,\dots,m_l}^l$ . We fix the generator. To derive the update for the discriminator, we need the state when it is fed with the training data, i.e.

$$\begin{aligned}
\rho_{\text{out}}^D(t + \epsilon) &= \text{tr}_{\text{in}(D)+\text{hid}} \left( e^{i\epsilon K_{m_{L+1}}^{L+1}} U_{m_{L+1}}^{L+1} \dots e^{i\epsilon K_1^{g+1}} U_1^{g+1} (|\phi^T\rangle \langle \phi^T| \otimes |0\dots 0\rangle \langle 0\dots 0|) \right. \\
&\quad \left. U_1^{g+1\dagger} e^{-i\epsilon K_1^{g+1}} \dots U_{m_{L+1}}^{L+1\dagger} e^{-i\epsilon K_{m_{L+1}}^{L+1}} \right)
\end{aligned}$$

$$\begin{aligned}
&= \rho_{\text{out}}^D(t) + i\epsilon \text{tr}_{\text{in(D)+hid}} \left( [K_{m_{L+1}}^{L+1}, U_{m_{L+1}}^{L+1} \dots U_1^{g+1} (|\phi^T\rangle \langle \phi^T| \otimes |0\dots 0\rangle \langle 0\dots 0|) \right. \\
&\quad U_1^{g+1\dagger} \dots U_{m_{L+1}}^{L+1\dagger}] + \dots + U_{m_{L+1}}^{L+1} \dots U_2^{g+1} [K_1^{g+1}, U_1^{g+1} |\phi^T\rangle \langle \phi^T| \\
&\quad \otimes |0\dots 0\rangle \langle 0\dots 0| U_1^{g+1\dagger}] U_2^{g+1\dagger} \dots U_{m_{L+1}}^{L+1\dagger} \left. \right) + \mathcal{O}(\epsilon^2),
\end{aligned}$$

and for the case it gets an input state from the generator, that is

$$\begin{aligned}
\rho_{\text{out}}^{G+D}(t + \epsilon) &= \text{tr}_{\text{in(G)+hid}} \left( e^{i\epsilon K_{m_{L+1}}^{L+1}} U_{m_{L+1}}^{L+1} \dots e^{i\epsilon K_1^{g+1}} U_1^{g+1} U_{m_g}^g \dots U_1^1 (|\psi_x^{\text{in}}\rangle \langle \psi_x^{\text{in}}| \right. \\
&\quad \otimes |0\dots 0\rangle \langle 0\dots 0|) U_1^{1\dagger} \dots U_{m_g}^{g\dagger} U_1^{g+1\dagger} e^{-i\epsilon K_1^{g+1}} \dots U_{m_{L+1}}^{L+1\dagger} e^{-i\epsilon K_{m_{L+1}}^{L+1}} \left. \right) \\
&= \rho_{\text{out}}^D(t) + i\epsilon \text{tr}_{\text{in(G)+hid}} \left( [K_{m_{L+1}}^{L+1}, U_{m_{L+1}}^{L+1} \dots U_1^1 (|\psi_x^{\text{in}}\rangle \langle \psi_x^{\text{in}}| \right. \\
&\quad \otimes |0\dots 0\rangle \langle 0\dots 0|) U_1^{1\dagger} \dots U_{m_{L+1}}^{L+1\dagger}] + \dots \\
&\quad + U_{m_{L+1}}^{L+1} \dots U_2^{g+1} [K_1^{g+1}, U_1^{g+1} U_{m_g}^g \dots U_1^1 (|\psi_x^{\text{in}}\rangle \langle \psi_x^{\text{in}}| \otimes |0\dots 0\rangle \langle 0\dots 0|) \\
&\quad U_1^{1\dagger} \dots U_{m_g}^{g\dagger} U_1^{g+1\dagger}] U_2^{g+1\dagger} \dots U_{m_{L+1}}^{L+1\dagger} \left. \right) \\
&\quad + \mathcal{O}(\epsilon^2).
\end{aligned}$$

The derivative of the discriminator loss function has the following form:

$$\begin{aligned}
\frac{d\mathcal{L}_D}{dt} &= \lim_{\epsilon \rightarrow 0} \frac{\mathcal{L}_D(t) + i\epsilon \frac{1}{S} \sum_{x=1}^S \langle 1| \text{tr}_{\text{in+hid}}(\dots) |1\rangle - \mathcal{L}_D(t)}{\epsilon} \\
&= \frac{i}{S} \sum_{x=1}^S \text{tr}_{\text{in+hid}} \left( \mathbb{1}_{\text{in+hid}} \otimes |1\rangle \langle 1| \left( \left( [K_{m_{L+1}}^{L+1}, U_{m_{L+1}}^{L+1} \dots U_1^{g+1} |\phi^T\rangle \langle \phi^T| \right. \right. \right. \\
&\quad \otimes |0\dots 0\rangle \langle 0\dots 0| U_1^{g+1\dagger} \dots U_{m_{L+1}}^{L+1\dagger}] + \dots \\
&\quad + U_{m_{L+1}}^{L+1} \dots U_2^{g+1} [K_1^{g+1}, U_1^{g+1} (|\phi^T\rangle \langle \phi^T| \otimes |0\dots 0\rangle \langle 0\dots 0|) U_1^{g+1\dagger}] \\
&\quad U_2^{g+1\dagger} \dots U_{m_{L+1}}^{L+1\dagger} \left. \right) \\
&\quad - \left( [K_{m_{L+1}}^{L+1}, U_{m_{L+1}}^{L+1} \dots U_1^1 (|\psi_x^{\text{in}}\rangle \langle \psi_x^{\text{in}}| \right. \\
&\quad \otimes |0\dots 0\rangle \langle 0\dots 0|) U_1^{1\dagger} \dots U_{m_{L+1}}^{L+1\dagger}] + \dots \\
&\quad + U_{m_{L+1}}^{L+1} \dots U_2^{g+1} [K_1^{g+1}, U_1^{g+1} U_{m_g}^g \dots U_1^1 (|\psi_x^{\text{in}}\rangle \langle \psi_x^{\text{in}}| \otimes |0\dots 0\rangle \langle 0\dots 0|) \\
&\quad U_1^{1\dagger} \dots U_{m_g}^{g\dagger} U_1^{g+1\dagger}] U_2^{g+1\dagger} \dots U_{m_{L+1}}^{L+1\dagger} \left. \right) \left. \right) \left. \right) \\
&= \frac{i}{S} \sum_{x=1}^S \text{tr}_{\text{in+hid}} \left( \right. \\
&\quad \left[ U_{m_{L+1}}^{L+1} \dots U_1^{g+1} (|\phi^T\rangle \langle \phi^T| \otimes |0\dots 0\rangle \langle 0\dots 0|) U_1^{g+1\dagger} \dots U_{m_{L+1}}^{L+1\dagger} \right. \\
&\quad \left. - U_{m_{L+1}}^{L+1} \dots U_1^1 (|\psi_x^{\text{in}}\rangle \langle \psi_x^{\text{in}}| \otimes |0\dots 0\rangle \langle 0\dots 0|) U_1^{1\dagger} \dots U_{m_{L+1}}^{L+1\dagger}, \right.
\end{aligned}$$

$$\begin{aligned}
& \mathbb{1}_{\text{in+hid}} \otimes |1\rangle \langle 1| \Big] K_{m_{L+1}}^{L+1} + \dots + \left[ U_1^{g+1} (|\phi^T\rangle \langle \phi^T| \otimes |0\dots 0\rangle \langle 0\dots 0|) U_1^{g+1\dagger} \right. \\
& \quad \left. - U_1^{g+1} U_{m_g}^g \dots U_1^1 (|\psi_x^{\text{in}}\rangle \langle \psi_x^{\text{in}}| \otimes |0\dots 0\rangle \langle 0\dots 0|) \right. \\
& \quad \left. U_1^{1\dagger} \dots U_{m_g}^{g\dagger} U_1^{g+1\dagger}, U_{m_{L+1}}^{L+1\dagger} \dots U_2^{g+1\dagger} \mathbb{1}_{\text{in+hid}} \otimes |1\rangle \langle 1| U_2^{g+1} \dots U_{m_{L+1}}^{L+1} \right] K_1^{g+1} \Big) \\
& = \frac{i}{S} \sum_{x=1}^S \text{tr}_{\text{in+hid}} \left( M_{m_{L+1}}^{L+1} K_{m_{L+1}}^{L+1} + \dots + M_1^{g+1} K_1^{g+1} \right).
\end{aligned}$$

Note that at this point  $|\phi^T\rangle \langle \phi^T| \otimes |0\dots 0\rangle \langle 0\dots 0|$  denotes  $\mathbb{1}_{\text{in}(G)+\text{hid}(G)} \otimes \otimes |\phi^T\rangle \langle \phi^T| \otimes |0\dots 0\rangle \langle 0\dots 0| \otimes \mathbb{1}_G \otimes \dots \otimes \mathbb{1}_G$ , to match the dimension of the other summand.

Until here we fixed the generator. Now we study the second part of the algorithm: the generator is fixed instead. Using the state

$$\begin{aligned}
\rho_{\text{out}2}^{G+D}(s + \epsilon) & = \text{tr}_{\text{in}(G)+\text{hid}} \left( U_{m_{L+1}}^{L+1} \dots U_1^{g+1} e^{i\epsilon K_{m_g}^g} U_{m_g}^g \dots e^{i\epsilon K_1^1} U_1^1 (|\psi_x^{\text{in}}\rangle \langle \psi_x^{\text{in}}| \right. \\
& \quad \left. \otimes |0\dots 0\rangle \langle 0\dots 0|) U_1^{1\dagger} e^{-i\epsilon K_1^1} \dots U_{m_g}^{g\dagger} e^{-i\epsilon K_{m_g}^g} U_1^{g+1\dagger} \dots U_{m_{L+1}}^{L+1\dagger} \right) \\
& = \rho_{\text{out}}^D(t) + i\epsilon \text{tr}_{\text{in}(G)+\text{hid}} \left( U_{m_{L+1}}^{L+1} \dots U_1^{g+1} [K_{m_g}^g, U_{m_g}^g \dots U_1^1 (|\psi_x^{\text{in}}\rangle \langle \psi_x^{\text{in}}| \right. \\
& \quad \left. \otimes |0\dots 0\rangle \langle 0\dots 0|) U_1^{1\dagger} \dots U_{m_g}^{g\dagger}] U_1^{g+1\dagger} \dots U_{m_{L+1}}^{L+1\dagger} + \dots \right. \\
& \quad \left. + U_{m_{L+1}}^{L+1} \dots U_2^1 [K_1^1, U_1^1 (|\psi_x^{\text{in}}\rangle \langle \psi_x^{\text{in}}| \otimes |0\dots 0\rangle \langle 0\dots 0|) U_1^{1\dagger}] U_2^{1\dagger} \dots U_{m_{L+1}}^{L+1\dagger} \right) \\
& \quad + \mathcal{O}(\epsilon^2)G
\end{aligned}$$

the derivative of the loss function for training the generator becomes

$$\begin{aligned}
\frac{d\mathcal{L}_G}{dt} & = \lim_{\epsilon \rightarrow 0} \frac{\mathcal{L}_G(t) + i\epsilon \frac{1}{S} \sum_x \langle 1| \text{tr}_{\text{in+hid}}(\dots) |1\rangle - \mathcal{L}_G(t)}{\epsilon} \\
& = \frac{i}{S} \sum_{x=1}^S \text{tr} \left( \mathbb{1}_{\text{in+hid}} \otimes |1\rangle \langle 1| \left( \left( U_{m_{l+1}}^{l+1} \dots U_1^{g+1} [K_{m_g}^g, U_{m_g}^g \dots U_1^1 (|\psi_x^{\text{in}}\rangle \langle \psi_x^{\text{in}}| \right. \right. \right. \\
& \quad \left. \left. \left. \otimes |0\dots 0\rangle \langle 0\dots 0|) U_1^{1\dagger} \dots U_{m_g}^{g\dagger}] U_1^{g+1\dagger} \dots U_{m_{l+1}}^{l+1\dagger} + \dots \right. \right. \right. \\
& \quad \left. \left. \left. + U_{m_{l+1}}^{l+1} \dots U_2^1 [K_1^1, U_1^1 (|\psi_x^{\text{in}}\rangle \langle \psi_x^{\text{in}}| \otimes |0\dots 0\rangle \langle 0\dots 0|) U_1^{1\dagger}] U_2^{1\dagger} \dots U_{m_{l+1}}^{l+1\dagger} \right) \right) \right) \\
& = \frac{i}{S} \sum_{x=1}^S \text{tr} \left( \right. \\
& \quad \left[ U_{m_g}^g \dots U_1^1 (|\psi_x^{\text{in}}\rangle \langle \psi_x^{\text{in}}| \otimes |0\dots 0\rangle \langle 0\dots 0|) U_1^{1\dagger} \dots U_{m_g}^{g\dagger}, \right. \\
& \quad \left. U_1^{g+1\dagger} \dots U_{m_{l+1}}^{l+1\dagger} (\mathbb{1}_{\text{in+hid}} \otimes |1\rangle \langle 1|) U_{m_{l+1}}^{l+1} \dots U_1^{g+1} \right] K_{m_g}^g + \dots \\
& \quad + \left[ U_1^1 (|\psi_x^{\text{in}}\rangle \langle \psi_x^{\text{in}}| \otimes |0\dots 0\rangle \langle 0\dots 0|) U_1^{1\dagger}, \right. \\
& \quad \left. U_2^{1\dagger} \dots U_{m_{l+1}}^{l+1\dagger} (\mathbb{1}_{\text{in+hid}} \otimes |1\rangle \langle 1|) U_{m_{l+1}}^{l+1} \dots U_2^1 \right] K_1^1 \Big)
\end{aligned}$$

$$\equiv \frac{i}{S} \sum_{x=1}^S \text{tr} \left( M_{m_g}^g K_{m_g}^g + \dots + M_1^1 K_1^1 \right).$$

In both updates, we parametrise the parameter matrices analogously as

$$K_j^l(t) = \sum_{\alpha_1, \alpha_2, \dots, \alpha_{m_{l-1}}, \beta} K_{j, \alpha_1, \dots, \alpha_{m_{l-1}}, \beta}^l(t) \left( \sigma^{\alpha_1} \otimes \dots \otimes \sigma^{\alpha_{m_{l-1}}} \otimes \sigma^\beta \right),$$

where the  $\alpha_i$  denote the qubits in the previous layer and  $\beta$  denotes the current qubit in layer  $l$ . To achieve the maximum of the loss function as a function of the parameters *fastest*, we maximise  $\frac{d\mathcal{L}}{dt}$ . Since this is a linear function, the extrema are at  $\pm\infty$ . To ensure that we get a finite solution, we introduce a Lagrange multiplier  $\lambda \in \mathbb{R}$ . Hence, to find  $K_j^l$  we have to solve the following maximisation problem (here for the discriminator update, the update for the generator is analogous):

$$\begin{aligned} & \max_{K_{j, \alpha_1, \dots, \beta}^l} \left( \frac{dC(t)}{dt} - \lambda \sum_{\alpha_i, \beta} K_{j, \alpha_1, \dots, \beta}^l(t)^2 \right) \\ &= \max_{K_{j, \alpha_1, \dots, \beta}^l} \left( \frac{i}{S} \sum_{x=1}^S \text{tr} \left( M_{m_{L+1}}^{L+1} K_{m_{L+1}}^{L+1} + \dots + M_1^{g+1} K_1^{g+1} \right) - \lambda \sum_{\alpha_1, \dots, \beta} K_{j, \alpha_1, \dots, \beta}^l(t)^2 \right) \\ &= \max_{K_{j, \alpha_1, \dots, \beta}^l} \left( \frac{i}{S} \sum_{x=1}^S \text{tr}_{\alpha_1, \dots, \beta} \left( \text{tr}_{\text{rest}} \left( M_{m_{L+1}}^{L+1} K_{m_{L+1}}^{L+1} + \dots + M_1^{g+1} K_1^{g+1} \right) \right) \right. \\ & \quad \left. - \lambda \sum_{\alpha_1, \dots, \beta} K_{j, \alpha_1, \dots, \beta}^l(t)^2 \right). \end{aligned}$$

Taking the derivative with respect to  $K_{j, \alpha_1, \dots, \beta}^l$  yields

$$\frac{i}{S} \sum_{x=1}^S \text{tr}_{\alpha_1, \dots, \beta} \left( \text{tr}_{\text{rest}} \left( M_j^l(t) \right) \left( \sigma^{\alpha_1} \otimes \dots \otimes \sigma^\beta \right) \right) - 2\lambda K_{j, \alpha_1, \dots, \beta}^l(t) = 0,$$

hence,

$$K_{j, \alpha_1, \dots, \beta}^l(t) = \frac{i}{2S\lambda} \sum_{x=1}^S \text{tr}_{\alpha_1, \dots, \beta} \left( \text{tr}_{\text{rest}} \left( M_j^l(t) \right) \left( \sigma^{\alpha_1} \otimes \dots \otimes \sigma^\beta \right) \right)$$

This yields the matrix

$$\begin{aligned} K_j^l(t) &= \sum_{\alpha_1, \dots, \beta} K_{j, \alpha_1, \dots, \beta}^l(t) \left( \sigma^{\alpha_1} \otimes \dots \otimes \sigma^\beta \right) \\ &= \frac{i}{2S\lambda} \sum_{\alpha_1, \dots, \beta} \sum_{x=1}^S \text{tr}_{\alpha_1, \dots, \beta} \left( \text{tr}_{\text{rest}} \left( M_j^l(t) \right) \left( \sigma^{\alpha_1} \otimes \dots \otimes \sigma^\beta \right) \right) \left( \sigma^{\alpha_1} \otimes \dots \otimes \sigma^\beta \right) \end{aligned}$$

$$= \frac{\eta 2^{m_{l-1} i}}{2S} \sum_{x=1}^S \text{tr}_{\text{rest}} \left( M_j^l(t) \right),$$

where  $\eta = 1/\lambda$  is the learning rate and  $\text{tr}_{\text{rest}}$  traces out all qubits that the perceptron unitary  $U_j^l$  does not act on.

Notice again that  $K_j^l$  updates the generator, if  $j \leq g$  for the number of layers  $g$  of the generator. The definition of  $M_j^l$  is

$$M_j^l = \left[ U_j^l \dots U_1^1 (|\psi_x^{\text{in}}\rangle \langle \psi_x^{\text{in}}| \otimes |0\dots 0\rangle \langle 0\dots 0|) U_1^{1\dagger} \dots U_j^{l\dagger}, \right. \\ \left. U_{j+1}^{l\dagger} \dots U_{m_{L+1}}^{L+1\dagger} (\mathbb{1}_{\text{in+hid}} \otimes |1\rangle \langle 1|) U_{m_{L+1}}^{L+1} \dots U_{l+1}^l \right]$$

for  $l \leq g$  and

$$M_j^l = \left[ U_j^l \dots U_1^{g+1} (|\phi^T\rangle \langle \phi^T| \otimes |0\dots 0\rangle \langle 0\dots 0|) U_1^{g+1\dagger} \dots U_j^{l\dagger} \right. \\ \left. - U_j^l \dots U_1^{g+1} U_{m_g}^g \dots U_1^1 (|\psi_x^{\text{in}}\rangle \langle \psi_x^{\text{in}}| \otimes |0\dots 0\rangle \langle 0\dots 0|) U_1^{1\dagger} \dots U_{m_g}^{g\dagger} U_1^{g+1\dagger} \dots U_j^{l\dagger}, \right. \\ \left. U_{j+1}^{l\dagger} \dots U_{m_{L+1}}^{L+1\dagger} (\mathbb{1}_{\text{in+hid}} \otimes |1\rangle \langle 1|) U_{m_{L+1}}^{L+1} \dots U_{l+1}^l \right]$$

else. □

## B Implementation of the DQNN<sub>Q</sub> as a PQC

The DQNN<sub>Q</sub> intends to realise each neuron as a separate qubit. Thus, implementing the DQNN<sub>Q</sub> as a quantum circuit requires  $M = \sum_{l=0}^{L+1} m_l$  qubits. This results in a  $2^M$ -dimensional Hilbert space  $\mathcal{H}^{\otimes M}$  which is the tensor product of  $M$  single qubit Hilbert spaces.

The main task of implementing the DQNN described by Eq. (1) is to find an appropriate realisation of the quantum perceptron  $U_j^l$  which is a general unitary acting on  $m_{l-1} + 1$  qubits. For the simulation on a classical computer it is sufficient to abstractly define the unitary matrix and update its entries during the training. However, to execute the DQNN on a quantum computer, a concrete realisation in the form of parameterised quantum gates is necessary to build. Once the parameterised quantum gates for representing the quantum perceptron are chosen, the full PQC can be built by composing the respective quantum perceptrons from all layers. When thinking about possible candidates for parameterised quantum gates, two objectives have to be well-balanced: on the one hand, the final realisation of the quantum perceptron should be as universal as possible, while on the other hand, the number of quantum gates and parameters should be kept as small as possible. If either one of these objectives is neglected, the DQNN<sub>Q</sub> will not perform as well as its classically simulated model.

Any arbitrary two-qubit unitary can be expressed by a two-qubit canonical gate and twelve single-qubit gates [66]. The two-qubit canonical gate is defined via three param-

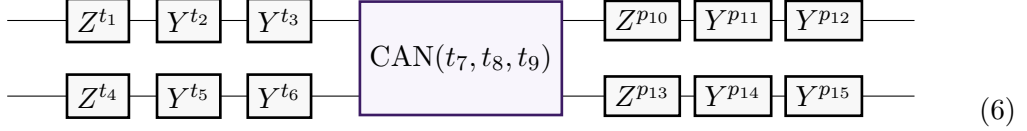
eters as:

$$\begin{aligned} \text{CAN}(t_x, t_y, t_z) &= e^{-i\frac{\pi}{2}t_x X \otimes X} e^{-i\frac{\pi}{2}t_y Y \otimes Y} e^{-i\frac{\pi}{2}t_z Z \otimes Z} \\ &= \text{RXX}(t_x \pi) \text{RYY}(t_y \pi) \text{RZZ}(t_z \pi) \end{aligned} \quad (4)$$

where  $X = \begin{pmatrix} 0 & 1 \\ 1 & 0 \end{pmatrix}$ ,  $Y = \begin{pmatrix} 0 & -i \\ i & 0 \end{pmatrix}$ ,  $Z = \begin{pmatrix} 1 & 0 \\ 0 & -1 \end{pmatrix}$  are the Pauli matrices, the RXX/RYY/RZZ gates are parameterised two qubit gates commonly available in quantum computing libraries, and  $t_{x,y,z} \in \mathbb{R}$  are the parameters. The necessary single qubit gates are parameterised Pauli- $Y$  and Pauli- $Z$  operators. These are equivalent to the following rotations around the  $y$ - and the  $z$ -axis:

$$\begin{aligned} Y^t &\simeq R_Y(\pi t) = e^{-i\frac{\pi}{2}tY} \\ Z^t &\simeq R_Z(\pi t) = e^{-i\frac{\pi}{2}tZ} \end{aligned} \quad (5)$$

up to a phase factor which is indicated by  $\simeq$ . By executing the two-qubit canonical gate in addition to prepending and appending three single qubit gates to each qubit in the following form:



any arbitrary two-qubit gate can be performed. As a graphical simplification, the used sequence  $Z$ - $Y$ - $Z$  of single-qubit gates can be expressed as the commonly used single qubit gate  $u(t_1, t_2, t_3)$ :

$$u(t_1, t_2, t_3) = R_Z(t_2)R_Y(t_1)R_Z(t_3) = \begin{pmatrix} \cos(t_1/2) & -e^{it_3} \sin(t_1/2) \\ e^{it_2} \sin(t_1/2) & e^{i(t_2+t_3)} \cos(t_1/2) \end{pmatrix} \quad (7)$$

where the different parameterisation compared to Eq. (5) should be noted.

The quantum perceptron is not, in general, a two-qubit unitary. Therefore the universal two-qubit gate from 6 can not directly be used. When thinking about implementing the universal two-qubit gate, it is helpful to think about the task fulfilled by the quantum perceptron, which is to process the states of its input qubits and change the output qubit's state accordingly. This motivates the application of separate two-qubit gates on each input-output qubit pair. However, numerical studies have shown that it is sufficient and often advantageous to refrain from using the single-qubit sequence from Eq. (7) and only use the two-qubit canonical gate as the direct realisation of the quantum perceptrons. In addition to realising the entire layer unitary  $U^l$ , i.e., all quantum perceptrons corresponding to layer  $l$ , the three-parameter single-qubit gate  $u$  is prepended to all input qubits and appended to all output qubits. To append single-qubit gates on the input qubits is pointless, as these are no longer used. To prepend single-qubit gates on the input qubits has proven unnecessary in numerical studies.

The interpretation of the DQNN as a quantum circuit employing the previously dis-

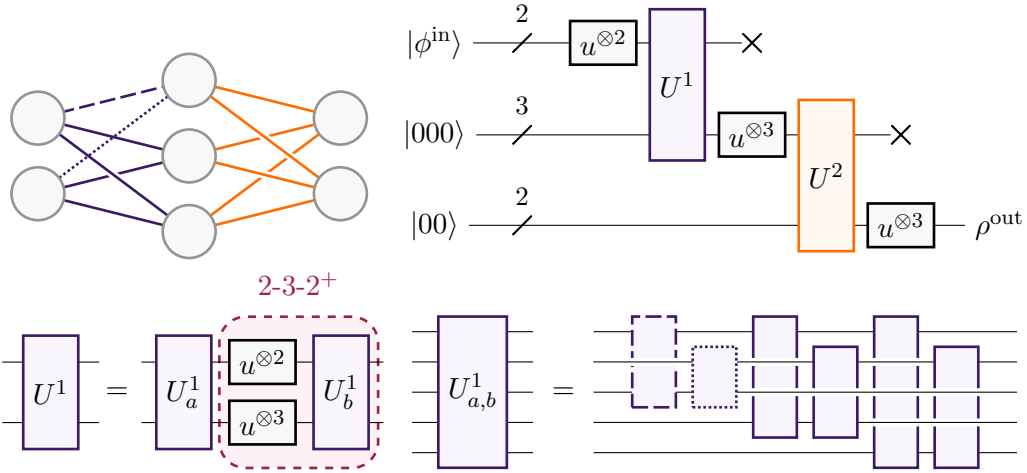


Figure 5: An exemplary  $\text{DQNN}_Q$  implementation as a parameterised quantum circuit suitable for the execution on NISQ devices. The unitaries  $U^l$  implement the layer-to-layer transition from the layer  $l-1$  to  $l$ . In the standard 2-3-2 network,  $U^l$  consists of  $m_{l-1} \cdot m_l$  two-qubit CAN gates. In the computationally more powerful 2-3-2<sup>+</sup> network,  $U^l$  features additional gates as shown in the pink dashed box.

cussed methods looks as follows. The first  $m_0$  qubits are initialised in a given, possibly mixed state  $\rho_{\text{in}}$ , while all remaining qubits are initialised in the computational basis state  $|0\rangle$ . The quantum circuit and the general  $\text{DQNN}_Q$  architecture are structured layer-wise and will therefore be described accordingly. The  $u$  gates are applied first, layer by layer ( $l = 1, \dots, L+1$ ), to the respective  $m_{l-1}$  input qubits. After that, the layer unitary  $U^l = \prod_{j=m_l}^1 U_j^l$  is applied to all input and output qubits. Here,  $U_j^l$  is a sequence of  $m_{l-1}$  CAN gates where the  $i^{\text{th}}$  CAN gate acts on the  $i^{\text{th}}$  input and the  $j^{\text{th}}$  output qubit. After each layer  $l$ , the  $m_{l-1}$  input qubits are neglected, i.e., they are just ignored for the rest of the quantum circuit. This layer's  $m_l$  output qubits serve as the input qubits for the next layer  $l+1$ . By this, the partial trace of Eq. (1) is realised. After the output layer  $L+1$ , again,  $u$  gates are applied to the remaining  $m$  output qubits. Thus, the quantum circuit consists of  $N_p = 3m + 3 \sum_{l=1}^{L+1} m_{l-1}(1 + m_l)$  parameters.

Due to the limitations of the current NISQ devices one is often interested in increasing the computational power of the  $\text{DQNN}_Q$  without using additional qubits. In this case, the quantum perceptron can be modified such that the  $\text{DQNN}_Q$ 's layer-to-layer transition gets computationally more powerful. This modification is denoted with a <sup>+</sup> as in 2-3-2<sup>+</sup>. The corresponding  $\text{DQNN}_Q$  is defined with the additional parameterised quantum gates shown in the pink dashed box in Fig. 5. The layer unitaries  $U_a^1$  and  $U_b^1$  share the same structure but are parameterised independently.

## C Further numerical results

In Section 3 we discussed the classical simulation of the DQGAN algorithm. In the following we extend the numerical examples of this section.

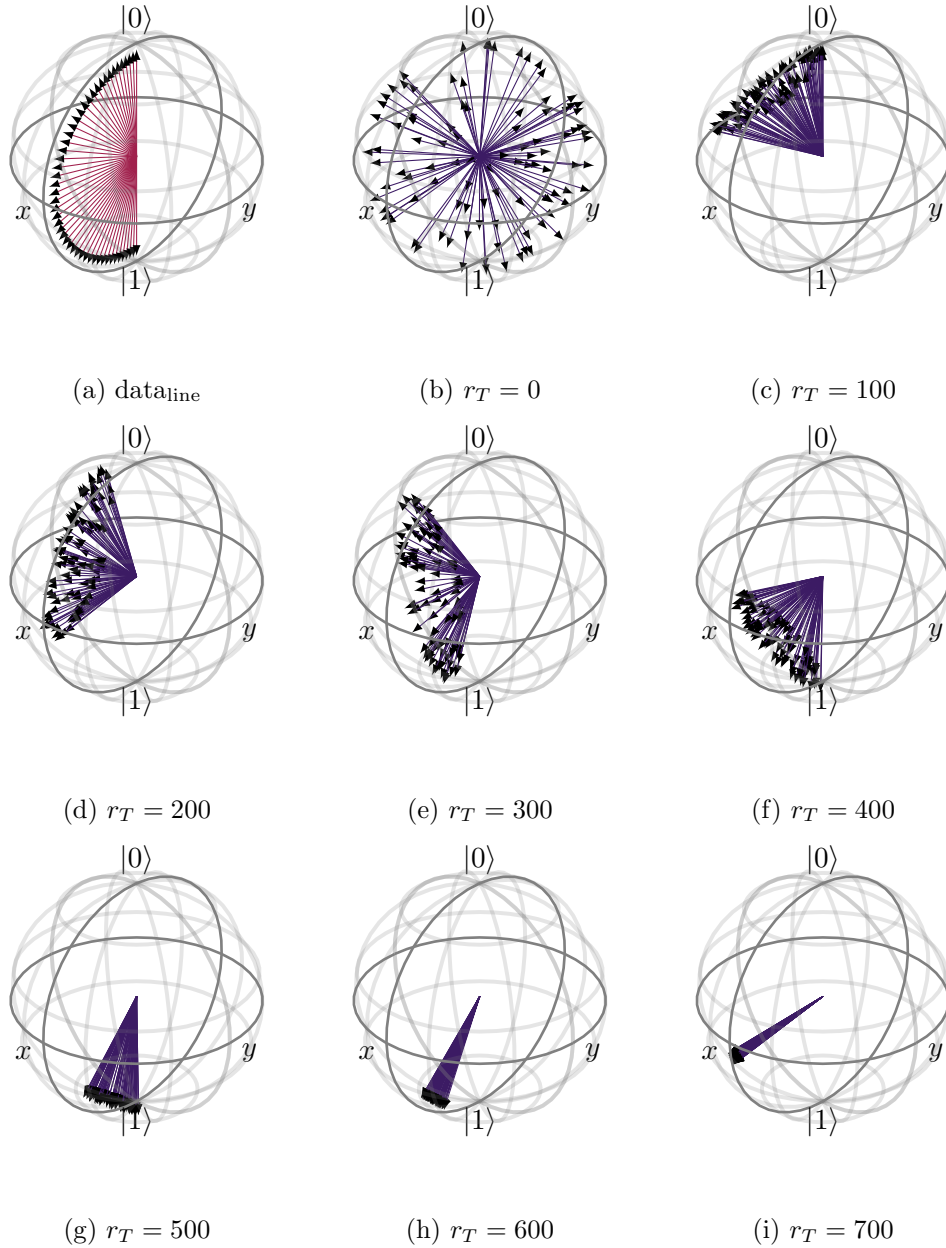


Figure 6: **Output of the generator.** To compare the output of the generator (b-i), during the training of a  $\circ-\circ-\circ$  DQGAN, to the data set  $\text{data}_{\text{line}}$  (a) we plot the states in Bloch spheres.

First of all, Fig. 6 gives an overview of the generator’s different training situations following the training depicted in Fig. 3a. At every of these training steps we build a set of 100 by the generator produced states and plot them in a Bloch sphere.

Secondly, in we train a 1-3-1 DQGAN with the training data

$$\text{data}_{\text{line}'} = \left\{ \frac{(N-x)|000\rangle + (x-1)|001\rangle}{\|((N-x)|000\rangle + (x-1)|001\rangle)\|} \right\}_{x=1}^N,$$

for  $N = 50$ .

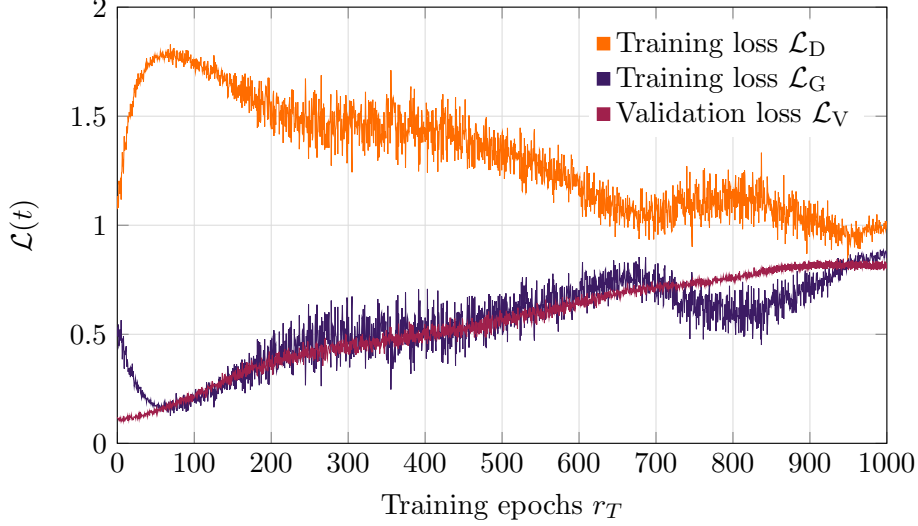
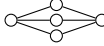
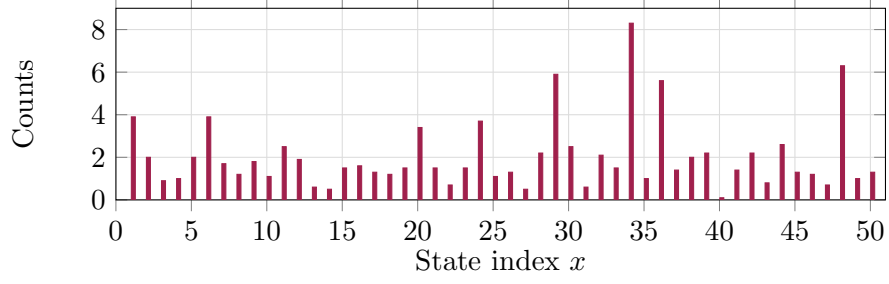


Figure 7: **Training a DQGAN.** The evolution of the training losses and validation loss during the training of a  DQGAN in  $r_T = 1000$  epochs with  $\eta = 1$  and  $\epsilon = 0.01$  using 50 data pairs of the data set  $\text{data}_{\text{line}'}$ , where 10 are used as training states.

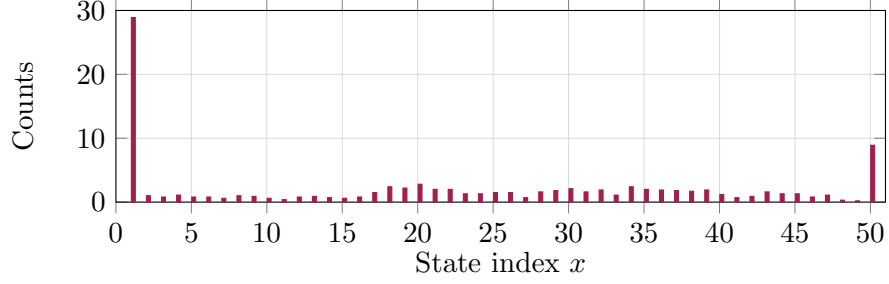
For a more comprehensive study, we averaged the histogram resulting after 200 training rounds using ten independent training attempts and 10 randomly chosen training states of  $\text{data}_{\text{line}'}$ . Fig. 8a shows that the diversity of the generator’s output is good, since all elements in  $\text{data}_{\text{line}'}$  get produced quite equally.

Moreover, we build an equivalent plot with the difference of choosing randomly 10 training states of  $\text{data}_{\text{cl}}$ , where

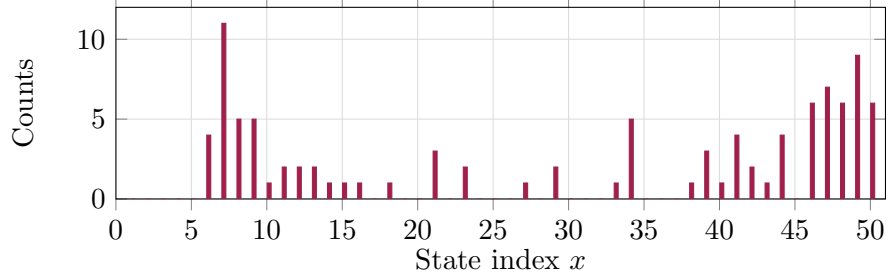
$$\text{data}_{\text{cl}} = \left\{ \frac{(2N-1)|0\rangle + (x-1)|1\rangle}{\|((2N-1)|0\rangle + (x-1)|1\rangle)\|} \right\}_{x=1}^{\frac{N}{2}} \cup \left\{ \frac{(2N-1)|0\rangle + (x-1)|1\rangle}{\|((2N-1)|0\rangle + (x-1)|1\rangle)\|} \right\}_{x=\frac{3N}{2}}^{2N}.$$



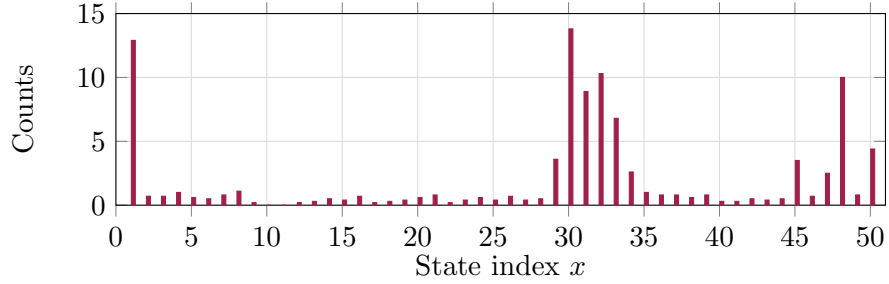
(a) Line trained with DQNN.



(b) Two clusters trained with DQNN.



(c) Two clusters trained with DQNN<sub>Q</sub>.



(d) Two clusters plus  $\frac{1}{\sqrt{2}}(|0\rangle + |1\rangle)$  trained with DQNN.

Figure 8: **Diversity analysis of a DQGAN.** This plot describes the output's diversity of a  $\circ-\circ-\circ$  DQGAN (DQGAN<sub>Q</sub>) trained in 200 epochs with  $\eta = 1$  ( $\eta_D = 0.5, \eta_G = 0.1$ ) and  $\epsilon = 0.01$  ( $\epsilon = 0.25$ ) using 10 quantum states of the data sets  $\text{data}_{\text{line}}$  (a),  $\text{data}_{\text{cl}}$  (b,c) and  $\text{data}_{\text{cl}+}$  (d) and compared the generator's output to the data set  $\text{data}_{\text{line}}$ .

Fig. 8b depicts the distribution of the generator’s output after 200 training epochs of ten training attempts with  $S = 10$  randomly chosen training states. The generator does not produce all elements in  $\text{data}_{\text{line}}$  equally often. Due to the average of ten independent training attempts, the states  $|0\rangle$  and  $|1\rangle$  are very prominent in this plot. Since the state  $|0\rangle$  is produced more often, we assume that the training states randomly chosen in every training attempt the  $S = 10$  training states were more often states of the first part of the cluster.

Further, by removing one state of the data set  $\text{data}_{\text{cl}}$  and replacing it by  $\frac{1}{\sqrt{2}}(|0\rangle + |1\rangle)$  we obtain the data set  $\text{data}_{\text{cl}+}$ . Fig. 8d shows the diversity of a generator resulting by training a DQGAN with  $\text{data}_{\text{cl}+}$ . We can see, that some states in the middle of the  $x$ -range are generated more often compared to the plot in Fig. 8b. However, the generator does not produce the state  $\frac{1}{\sqrt{2}}(|0\rangle + |1\rangle)$  ( $x = 25$ ) very often and the resulting peak in the histogram is rather shifted more in the direction of the  $|1\rangle$  state ( $x = 50$ ).

Additionally, we trained a  $\text{DQGAN}_{\text{Q}}$  using the clustered data set  $\text{data}_{\text{cl}}$  and tested the generator’s diversity after  $r_T = 200$  training epochs for a single execution on the  $\text{data}_{\text{line}}$ . The results are depicted in Fig. 8c which show the generator’s ability to extend the clustered training data while keeping its main characteristics. However, as opposed to the DQGAN simulated on a classical computer, the  $\text{DQGAN}_{\text{Q}}$  does not achieve to produce the full range of training data.